Received: 1 December 2020 | Revised: 31 August 2021 | Accepted: 1 October 2021

DOI: 10.1002/rnc.5849

SPECIAL ISSUE ARTICLE

WILEY

Adaptive PID control of robotic manipulators without equality/inequality constraints on control gains

Lei Qiao[1,2] | Min Zhao[1,2] | Chao Wu[1,2] | Tong Ge[1,2] | Rui Fan[3,4] | Weidong Zhang[5]

[1]State Key Laboratory of Ocean Engineering, Shanghai Jiao Tong University, Shanghai, China

[2]School of Naval Architecture, Ocean and Civil Engineering, Shanghai Jiao Tong University, Shanghai, China

[3]Department of Control Science and Engineering, College of Electronics and Information Engineering, Tongji University, Shanghai, China

[4]Shanghai Research Institute for Intelligent Autonomous Systems, Shanghai, China

[5]Department of Automation, Shanghai Jiao Tong University, Shanghai, China

Correspondence
Min Zhao, School of Naval Architecture, Ocean and Civil Engineering, Shanghai Jiao Tong University, Shanghai 200240, China.
Email: min.zhao@sjtu.edu.cn

Funding information
National Natural Science Foundation of China, Grant/Award Number: 52101365; LingChuang Research Project of China National Nuclear Corporation; Shanghai Sailing Program, Grant/Award Number: 21YF1419800; State Key Laboratory of Ocean Engineering (Shanghai Jiao Tong University), Grant/Award Number: GKZD010081; Young Talent Project of China National Nuclear Corporation

Abstract

This article proposes two novel adaptive PID controllers for the trajectory tracking of robotic manipulators with known or unknown upper bound of the uncertainties, respectively. The designed controllers are shown to be not only robust with respect to the uncertainties but also adaptive with reference to the unknown manipulator and load parameters. Lyapunov stability analysis is included to prove eventual local asymptotic tracking. The salient features of the two proposed adaptive PID controllers are as follows: (1) they guarantee the eventual asymptotic convergence of the manipulator joint position and velocity tracking errors to zero with no need of any equality/inequality constraints on the controller gains when compared with the classical PID controller and the existing adaptive PID controllers; and (2) they offer better robustness against uncertainties than the existing classical PID controller, the adaptive PD controller, the linear active disturbance rejection controller, and the nonlinear disturbance observer based adaptive PID controller. Simulation studies and comprehensive comparisons demonstrate the superiorities of the two proposed adaptive PID controllers.

KEYWORDS

adaptive PID control, robotic manipulators, trajectory tracking, without equality/inequality constraints

1 | INTRODUCTION

Trajectory tracking control of robotic manipulators is a challenging task due to the inherent nonlinear system dynamics, unknown manipulator and load parameters, and uncertainties.[1–3] Such control problem has received great attention of robot control theorists during the past decades. In the early stages, PID control is employed for tracking control of robotic manipulators. Due to that the PID algorithm is simple in structure and easy to implement, it has still been widely used in industrial applications in nowadays. Several important theoretical results in trajectory tracking control of robotic manipulators adopting classical PID algorithm are given in References 4–6. In Reference 4, it is shown that there exist

[Correction added on 17 November 2021, after first online publication: affiliation 1 has been corrected in this version.]

PID parameters which can guarantee the robotic manipulator to locally track a desired trajectory with arbitrary precision, provided that initial position and velocity errors are sufficiently small. In Reference 5, suitable Lyapunov functions are proposed to prove that there exist design parameters which can hold a locally asymptotically stable closed-loop system and stable trajectory tracking. In Reference 6, a novel PID control configuration derived from modeling error compensation ideas is proposed for position control of robot manipulators in joint space. The semiglobal stability of the proposed PID control law is proved, which depends only on the inertial parameters of the robot manipulators. However, it has been shown in Reference 7 that there are two main problems using the above classical PID controllers: (1) the PID gains should meet some inequality constraints to guarantee the local/semiglobal stability of the closed-loop system; and (2) the unknown manipulator and load parameters and uncertainties cannot be compensated for.

Adaptive technique is able to deal with system model uncertainties. This motivates to combine PD/PID algorithm with adaptive technique to address the trajectory tracking control problem of robotic manipulators with uncertain model parameters. In Reference 8, an adaptive PD controller is proposed for tracking control of robotic manipulators. The unknown manipulator and payload parameters can be estimated online and the global asymptotical stability with respect to the joint positions and velocities is able to be guaranteed. However, this adaptive PD controller may exhibit poor robustness to the other uncertainties such as friction, torque disturbance, and so on, since these uncertainties are not taken into account in the manipulator dynamic model. Some extensions of the above adaptive PD controller in the tracking control problem of robotic manipulators can refer to References 9–11. However, these controllers may also hold poor uncertainties rejection capability because the uncertainties are also not considered in the manipulator dynamics. Moreover, although some improvements are made by these controllers compared with the adaptive PD controller presented in Reference 8, additional inequality constraints on the controller gains are needed to ensure the global asymptotic stability of the closed-loop system.

Adaptive algorithm plus PID control for the trajectory tracking of robotic manipulators has limited research. In Reference 12, an adaptive PID control scheme which consists of adaptation mechanism, sliding mode control and supervisory control is proposed for robot manipulators. However, it only ensures the joint position and velocity tracking errors with H_∞ tracking performance instead of converging to zero. In Reference 13, two robust adaptive PID controllers are designed for the trajectory tracking control of robotic manipulators with known or unknown upper bound of the external disturbances, respectively. The two proposed controllers are shown to be valid not only in the presence of unknown manipulator and load parameters but also in the presence of time-varying external disturbances. Moreover, the asymptotic stable positions and velocities tracking are guaranteed. Nevertheless, to guarantee the locally asymptotic stability of the position and velocity tracking errors, an equality constraint on the controller gains is required, that is, for each controller, the integral gain must be equal to the differential gain.

Nowadays, adaptive technique combines with some advanced control methods have been proposed to solve the trajectory tracking control of robotic manipulators, the readers can refer to adaptive neural network control,[2,14–17] adaptive backstepping control,[18–20] adaptive iterative learning control,[21,22] adaptive sliding mode control,[3,23–25] adaptive fuzzy control,[26,27] and so forth. However, this study only devotes to investigate such a control structure consisting of only adaptive technique and classical PID control for the trajectory tracking control of robotic manipulators.

In this article, two new adaptive PID controllers are proposed to address the problem of trajectory tracking control of robotic manipulators in two cases that the upper bound of the uncertainties is known or unknown, respectively. The main contributions of this work are twofold.

1. By introducing an exponential convergent factor into the controllers design, the two proposed adaptive PID controllers can guarantee the eventual asymptotic convergence of the joint position and velocity tracking errors to zero meanwhile do not require any equality/inequality constraints on the controller gains, when compared to the classical PID controller, the adaptive PID controllers presented in Reference 12, and the adaptive PID controller presented in Reference 13.
2. With the effective compensation mechanism for the uncertainties existing in the manipulator dynamics, the two proposed adaptive PID controllers can provide better robustness to the uncertainties in contrast to the classical PID controller, the adaptive PD controller,[8] the linear active disturbance rejection controller (LADRC),[28,29] and the nonlinear disturbance observer (NDOB)[30] based adaptive PID controller.

The rest of this article is organized as follows. Section 2 formulates the robot manipulator dynamics and gives the control objective. Section 3 presents the two novel adaptive PID controllers design, the corresponding stability analysis, and some guidance to the controller parameters selection. Simulation verifications are performed in Section 4. Finally, conclusions are summarized in Section 5.

Notations. The following notations are used throughout this article. For a vector $\vartheta \in R^n$, its norm is defined as the Euclidean norm, that is, $\|\vartheta\| = \sqrt{\vartheta^T \vartheta}$. For a matrix $\boldsymbol{E} \in R^{n\times n}$, $\lambda_{\min}(\boldsymbol{E})$ and $\lambda_{\max}(\boldsymbol{E})$ are denoted as the smallest and largest eigenvalues of matrix $\boldsymbol{E}$, respectively. The norm of matrix $\boldsymbol{E}$ is defined as the induced 2-norm, that is, $\|\boldsymbol{E}\| = \sqrt{\lambda_{\max}\left(\boldsymbol{E}^T\boldsymbol{E}\right)}$.

2 | PROBLEM FORMULATION

The dynamic model of an n-link, revolute, rigid robotic manipulator with uncertainties can be described by[13,31]

$$\boldsymbol{M}(\boldsymbol{q})\ddot{\boldsymbol{q}} + \boldsymbol{C}(\boldsymbol{q}, \dot{\boldsymbol{q}})\dot{\boldsymbol{q}} + \boldsymbol{G}(\boldsymbol{q}) + \boldsymbol{u} = \boldsymbol{\tau}, \tag{1}$$

where $\boldsymbol{q}, \dot{\boldsymbol{q}}, \ddot{\boldsymbol{q}} \in R^n$ are the joint position, velocity, and acceleration vectors, respectively, $\boldsymbol{M}(\boldsymbol{q}) \in R^{n\times n}$ is the inertia matrix, $\boldsymbol{C}(\boldsymbol{q}, \dot{\boldsymbol{q}}) \in R^{n\times n}$ is the Coriolis and centripetal forces matrix, $\boldsymbol{G}(\boldsymbol{q}) \in R^n$ is the gravitational force vector, $\boldsymbol{\tau} \in R^n$ is the vector of applied joint inputs, and $\boldsymbol{u} \in R^n$ is the vector of uncertainties presenting friction, torque disturbance, and so forth.

Some properties of the manipulator dynamic model (1) are summarized as follows:

Property 1 (31). The inertial matrix $\boldsymbol{M}(\boldsymbol{q})$ is symmetric and positive definite. There exist positive constants m_m and m_M such that $m_m\|\xi\|^2 \le \xi^T\boldsymbol{M}(\boldsymbol{q})\xi \le m_M\|\xi\|^2, \forall \xi \in R^n$.

Property 2 Given the definition of $\boldsymbol{C}(\boldsymbol{q}, \dot{\boldsymbol{q}})$ as in Reference 8, the matrix $\dot{\boldsymbol{M}}(\boldsymbol{q}) - 2\boldsymbol{C}(\boldsymbol{q}, \dot{\boldsymbol{q}})$ is skew symmetric, which implies that $\xi^T[\dot{\boldsymbol{M}}(\boldsymbol{q}) - 2\boldsymbol{C}(\boldsymbol{q}, \dot{\boldsymbol{q}})]\xi = 0$ for $\forall \xi \in R^n$. Furthermore, $\dot{\boldsymbol{M}}(\boldsymbol{q}) = \boldsymbol{C}(\boldsymbol{q}, \dot{\boldsymbol{q}}) + \boldsymbol{C}^T(\boldsymbol{q}, \dot{\boldsymbol{q}})$.

Property 3 (8, 31, and 32). The matrices $\boldsymbol{M}(\boldsymbol{q})$, $\boldsymbol{C}(\boldsymbol{q}, \dot{\boldsymbol{q}})$, and $\boldsymbol{G}(\boldsymbol{q})$ are linear in terms of robot and load parameters such that

$$\boldsymbol{M}(\boldsymbol{q})\boldsymbol{\alpha} + \boldsymbol{C}(\boldsymbol{q}, \dot{\boldsymbol{q}})\boldsymbol{\beta} + \boldsymbol{G}(\boldsymbol{q}) = \boldsymbol{\Psi}(\boldsymbol{q}, \dot{\boldsymbol{q}}, \boldsymbol{\alpha}, \boldsymbol{\beta})\boldsymbol{P},$$

where $\boldsymbol{\Psi}(\boldsymbol{q}, \dot{\boldsymbol{q}}, \boldsymbol{\alpha}, \boldsymbol{\beta}) \in R^{n\times m}$ is a known regression matrix and $\boldsymbol{P} \in R^m$ is a constant vector of the unknown manipulator and load parameters.

Property 4 The Coriolis and centripetal forces matrix $\boldsymbol{C}(\boldsymbol{q}, \dot{\boldsymbol{q}})$ is bounded provided $\dot{\boldsymbol{q}}$ is bounded, that is, a positive constant k_c exists such that $\|\boldsymbol{C}(\boldsymbol{q}, \dot{\boldsymbol{q}})\| \le k_c$.

The control objective of this article is to design the adaptive PID controllers, such that the joint position and velocity vectors can eventually asymptotically track the desired trajectories, when the robotic manipulator is subject to parameter uncertainties and other uncertainties $\boldsymbol{u}$, at the same time no equality/inequality constraints on the controller gains are required.

3 | ADAPTIVE PID CONTROLLERS DESIGN

To attain the aforementioned control objective, two novel adaptive PID controllers are developed with known or unknown upper bound of the uncertainties, respectively. Before designing the controllers, we introduce two auxiliary vectors $\boldsymbol{x}$ and $\boldsymbol{q}_r$ as

$$\boldsymbol{x} = \dot{\tilde{\boldsymbol{q}}} + \gamma\tilde{\boldsymbol{q}}, \tag{2}$$

$$\dot{\boldsymbol{q}}_r = \dot{\boldsymbol{q}}_d - \gamma\tilde{\boldsymbol{q}}, \tag{3}$$

where $\boldsymbol{q}_d, \dot{\boldsymbol{q}}_d \in R^n$ are the desired joint position and velocity trajectories, respectively, $\tilde{\boldsymbol{q}} = \boldsymbol{q} - \boldsymbol{q}_d$ and $\dot{\tilde{\boldsymbol{q}}} = \dot{\boldsymbol{q}} - \dot{\boldsymbol{q}}_d$ are the joint position and velocity tracking errors, respectively, and γ is a positive constant.

From (2) and (3), we have

$$\dot{\boldsymbol{q}}_r = \dot{\boldsymbol{q}} - \boldsymbol{x}. \tag{4}$$

For Property 3, let $\boldsymbol{\alpha} = \ddot{\boldsymbol{q}}_r$, $\boldsymbol{\beta} = \dot{\boldsymbol{q}}_r$ we get

$$\boldsymbol{M}(\boldsymbol{q})\ddot{\boldsymbol{q}}_r + \boldsymbol{C}(\boldsymbol{q},\dot{\boldsymbol{q}})\dot{\boldsymbol{q}}_r + \boldsymbol{G}(\boldsymbol{q}) = \boldsymbol{\Psi}\left(\boldsymbol{q},\dot{\boldsymbol{q}},\dot{\boldsymbol{q}}_r,\ddot{\boldsymbol{q}}_r\right)\boldsymbol{P}. \tag{5}$$

Substituting (4) into (5) yields

$$\boldsymbol{M}(\boldsymbol{q})\ddot{\boldsymbol{q}} + \boldsymbol{C}(\boldsymbol{q},\dot{\boldsymbol{q}})\dot{\boldsymbol{q}} + \boldsymbol{G}(\boldsymbol{q}) - \boldsymbol{M}(\boldsymbol{q})\dot{\boldsymbol{x}} - \boldsymbol{C}(\boldsymbol{q},\dot{\boldsymbol{q}})\boldsymbol{x} = \boldsymbol{\Psi}\left(\boldsymbol{q},\dot{\boldsymbol{q}},\dot{\boldsymbol{q}}_r,\ddot{\boldsymbol{q}}_r\right)\boldsymbol{P}. \tag{6}$$

To develop the controllers, we make the following assumptions.

Assumption 1. The desired joint position, velocity, and acceleration trajectories $\boldsymbol{q}_d$, $\dot{\boldsymbol{q}}_d$, and $\ddot{\boldsymbol{q}}_d$ are available and bounded.

The uncertainties $\boldsymbol{u}$ are the collection of the friction, residual time-varying disturbances, and so on. As mentioned in Reference 32, the viscous and Coulomb friction forces may be modeled as $\boldsymbol{F}_v\dot{\boldsymbol{q}} + \boldsymbol{F}_c\text{sgn}(\dot{\boldsymbol{q}})$, so the uncertainties are functions of the system states and may grow beyond any constant bound if the system becomes unstable. Therefore, the bound of the uncertainties $\boldsymbol{u}$ is assumed the same as in References 32 and 33 such that:

Assumption 2 (32 and 33). The uncertainty effects $\boldsymbol{u}$ are bounded in the following manner:

$$\|\boldsymbol{u}\| \le b_0 + b_1\|\dot{\boldsymbol{q}}\| + b_2\|\boldsymbol{q}\|,$$

where b_i $(i = 0, 1, 2)$ are all positive constants.

3.1 | Controller design with known upper bound of the uncertainties

For the robotic manipulator systems (1), assume that the upper bound of the uncertainties $\boldsymbol{u}$ is known, then consider the following controller:

$$\boldsymbol{\tau} = -\boldsymbol{K}_P\tilde{\boldsymbol{q}} - \boldsymbol{K}_D\dot{\tilde{\boldsymbol{q}}} - \boldsymbol{K}_I\int_0^t \tilde{\boldsymbol{q}}dl + \boldsymbol{\Psi}\left(\boldsymbol{q},\dot{\boldsymbol{q}},\dot{\boldsymbol{q}}_r,\ddot{\boldsymbol{q}}_r\right)\hat{\boldsymbol{P}} + \boldsymbol{\Lambda}, \tag{7}$$

where $\boldsymbol{K}_P, \boldsymbol{K}_D, \boldsymbol{K}_I \in R^{n\times n}$ are symmetric positive definite constant matrices, $\hat{\boldsymbol{P}}$ is the estimation of $\boldsymbol{P}$ and it is updated by the following adaptation law:

$$\begin{cases} \dot{\hat{\boldsymbol{P}}} = -\boldsymbol{\Phi}\boldsymbol{\Psi}^T\left(\boldsymbol{q},\dot{\boldsymbol{q}},\dot{\boldsymbol{q}}_r,\ddot{\boldsymbol{q}}_r\right)(\boldsymbol{x}+\varepsilon\tilde{\boldsymbol{q}}), \\ \varepsilon = \lambda e^{-\gamma t} \text{ with } \gamma,\ \lambda = \text{const} > 0, \end{cases} \tag{8}$$

in which $\boldsymbol{\Phi} \in R^{m\times m}$ is a symmetric positive definite constant matrix that determines the rate of adaptation, and $\boldsymbol{\Lambda}$ is the compensation term which is given by

$$\boldsymbol{\Lambda} = -\left[b_0 + b_1\|\dot{\boldsymbol{q}}\| + b_2\|\boldsymbol{q}\| + \|\boldsymbol{K}_I\|\left\|\int_0^t \tilde{\boldsymbol{q}}dl\right\|\right]\text{sgn}(\boldsymbol{x}+\varepsilon\tilde{\boldsymbol{q}}), \tag{9}$$

in which the vector $\text{sgn}(\boldsymbol{x}+\varepsilon\tilde{\boldsymbol{q}})$ is obtained by applying the signum function to all elements of $\boldsymbol{x}+\varepsilon\tilde{\boldsymbol{q}}$.

Theorem 1. Given the robotic manipulator dynamics (1) with known upper bound of the uncertainties $\boldsymbol{u}$ controlled by the controller (7)–(9), the position and velocity tracking errors $\tilde{\boldsymbol{q}}$ and $\dot{\tilde{\boldsymbol{q}}}$ eventually asymptotically converge to zero locally, and the parameter estimation error $\tilde{\boldsymbol{P}} = \hat{\boldsymbol{P}} - \boldsymbol{P}$ is eventually bounded.

Proof. Consider the following Lyapunov candidate function:

$$V = \frac{1}{2}\boldsymbol{\eta}^T\boldsymbol{H}\boldsymbol{\eta} + \frac{1}{2}\tilde{\boldsymbol{P}}^T\boldsymbol{\Phi}^{-1}\tilde{\boldsymbol{P}}, \tag{10}$$

where

$$\boldsymbol{\eta} = \begin{bmatrix}\boldsymbol{x}\\ \tilde{\boldsymbol{q}}\end{bmatrix}, \boldsymbol{H} = \begin{bmatrix}\boldsymbol{M}(\boldsymbol{q}) & \varepsilon\boldsymbol{M}(\boldsymbol{q})\\ \varepsilon\boldsymbol{M}(\boldsymbol{q}) & \boldsymbol{K}_F\end{bmatrix} \text{ with } \boldsymbol{K}_F = (\gamma+\varepsilon)\boldsymbol{K}_D + \boldsymbol{K}_P.$$

It has been shown in Reference 9 that, if ε ($\varepsilon > 0$) is small enough such that $\lambda_{\min}(\boldsymbol{K}_F)/m_M > \varepsilon^2$, the matrix $\boldsymbol{H}$ is symmetric positive definite and consequently $V > 0$.

Then, the time derivative of V can be written as

$$\begin{aligned}\dot{V} = {} & \boldsymbol{x}^T\boldsymbol{M}(\boldsymbol{q})\dot{\boldsymbol{x}} + \frac{1}{2}\boldsymbol{x}^T\dot{\boldsymbol{M}}(\boldsymbol{q})\boldsymbol{x} + \dot{\varepsilon}\boldsymbol{x}^T\boldsymbol{M}(\boldsymbol{q})\widetilde{\boldsymbol{q}} + \varepsilon\dot{\boldsymbol{x}}^T\boldsymbol{M}(\boldsymbol{q})\widetilde{\boldsymbol{q}} \\ & + \varepsilon\boldsymbol{x}^T\dot{\boldsymbol{M}}(\boldsymbol{q})\widetilde{\boldsymbol{q}} + \varepsilon\boldsymbol{x}^T\boldsymbol{M}(\boldsymbol{q})\dot{\widetilde{\boldsymbol{q}}} + \widetilde{\boldsymbol{q}}^T\boldsymbol{K}_P\dot{\widetilde{\boldsymbol{q}}} + \gamma\widetilde{\boldsymbol{q}}^T\boldsymbol{K}_D\dot{\widetilde{\boldsymbol{q}}} \\ & + \varepsilon\widetilde{\boldsymbol{q}}^T\boldsymbol{K}_D\dot{\widetilde{\boldsymbol{q}}} + \frac{1}{2}\dot{\varepsilon}\widetilde{\boldsymbol{q}}^T\boldsymbol{K}_D\widetilde{\boldsymbol{q}} + \widetilde{\boldsymbol{P}}^T\boldsymbol{\Phi}^{-1}\dot{\widetilde{\boldsymbol{P}}}.\end{aligned} \tag{11}$$

Substituting (1) and (6) into (11) yields

$$\begin{aligned}\dot{V} = {} & \frac{1}{2}\boldsymbol{x}^T\dot{\boldsymbol{M}}(\boldsymbol{q})\boldsymbol{x} + \dot{\varepsilon}\boldsymbol{x}^T\boldsymbol{M}(\boldsymbol{q})\widetilde{\boldsymbol{q}} + \varepsilon\boldsymbol{x}^T\dot{\boldsymbol{M}}(\boldsymbol{q})\widetilde{\boldsymbol{q}} \\ & + \varepsilon\boldsymbol{x}^T\boldsymbol{M}(\boldsymbol{q})\dot{\widetilde{\boldsymbol{q}}} + \widetilde{\boldsymbol{q}}^T\boldsymbol{K}_P\dot{\widetilde{\boldsymbol{q}}} + \gamma\widetilde{\boldsymbol{q}}^T\boldsymbol{K}_D\dot{\widetilde{\boldsymbol{q}}} \\ & + \varepsilon\widetilde{\boldsymbol{q}}^T\boldsymbol{K}_D\dot{\widetilde{\boldsymbol{q}}} + \frac{1}{2}\dot{\varepsilon}\widetilde{\boldsymbol{q}}^T\boldsymbol{K}_D\widetilde{\boldsymbol{q}} + \widetilde{\boldsymbol{P}}^T\boldsymbol{\Phi}^{-1}\dot{\widetilde{\boldsymbol{P}}} \\ & + \boldsymbol{x}^T\left[\boldsymbol{\tau} - \boldsymbol{u} - \boldsymbol{C}(\boldsymbol{q},\dot{\boldsymbol{q}})\boldsymbol{x} - \boldsymbol{\Psi}\left(\boldsymbol{q},\dot{\boldsymbol{q}},\dot{\boldsymbol{q}}_r,\ddot{\boldsymbol{q}}_r\right)\boldsymbol{P}\right] \\ & + \varepsilon\widetilde{\boldsymbol{q}}^T\left[\boldsymbol{\tau} - \boldsymbol{u} - \boldsymbol{C}(\boldsymbol{q},\dot{\boldsymbol{q}})\boldsymbol{x} - \boldsymbol{\Psi}\left(\boldsymbol{q},\dot{\boldsymbol{q}},\dot{\boldsymbol{q}}_r,\ddot{\boldsymbol{q}}_r\right)\boldsymbol{P}\right].\end{aligned} \tag{12}$$

From the control law (7), we have

$$\begin{aligned} & \boldsymbol{x}^T\left[\boldsymbol{\tau} - \boldsymbol{u} - \boldsymbol{C}(\boldsymbol{q},\dot{\boldsymbol{q}})\boldsymbol{x} - \boldsymbol{\Psi}\left(\boldsymbol{q},\dot{\boldsymbol{q}},\dot{\boldsymbol{q}}_r,\ddot{\boldsymbol{q}}_r\right)\boldsymbol{P}\right] \\ & = -\boldsymbol{x}^T\boldsymbol{K}_P\widetilde{\boldsymbol{q}} - \boldsymbol{x}^T\boldsymbol{K}_D\dot{\widetilde{\boldsymbol{q}}} - \boldsymbol{x}^T\boldsymbol{K}_I\int_0^t\widetilde{\boldsymbol{q}}dl - \boldsymbol{x}^T\boldsymbol{C}(\boldsymbol{q},\dot{\boldsymbol{q}})\boldsymbol{x} \\ & \quad + \boldsymbol{x}^T\boldsymbol{\Psi}\left(\boldsymbol{q},\dot{\boldsymbol{q}},\dot{\boldsymbol{q}}_r,\ddot{\boldsymbol{q}}_r\right)\widetilde{\boldsymbol{P}} + \boldsymbol{x}^T\boldsymbol{\Lambda} - \boldsymbol{x}^T\boldsymbol{u},\end{aligned} \tag{13a}$$

$$\begin{aligned} & \varepsilon\widetilde{\boldsymbol{q}}^T\left[\boldsymbol{\tau} - \boldsymbol{u} - \boldsymbol{C}(\boldsymbol{q},\dot{\boldsymbol{q}})\boldsymbol{x} - \boldsymbol{\Psi}\left(\boldsymbol{q},\dot{\boldsymbol{q}},\dot{\boldsymbol{q}}_r,\ddot{\boldsymbol{q}}_r\right)\boldsymbol{P}\right] \\ & = -\varepsilon\widetilde{\boldsymbol{q}}^T\boldsymbol{K}_P\widetilde{\boldsymbol{q}} - \varepsilon\widetilde{\boldsymbol{q}}^T\boldsymbol{K}_D\dot{\widetilde{\boldsymbol{q}}} - \varepsilon\widetilde{\boldsymbol{q}}^T\boldsymbol{K}_I\int_0^t\widetilde{\boldsymbol{q}}dl - \varepsilon\widetilde{\boldsymbol{q}}^T\boldsymbol{C}(\boldsymbol{q},\dot{\boldsymbol{q}})\boldsymbol{x} \\ & \quad + \varepsilon\widetilde{\boldsymbol{q}}^T\boldsymbol{\Psi}\left(\boldsymbol{q},\dot{\boldsymbol{q}},\dot{\boldsymbol{q}}_r,\ddot{\boldsymbol{q}}_r\right)\widetilde{\boldsymbol{P}} + \varepsilon\widetilde{\boldsymbol{q}}^T\boldsymbol{\Lambda} - \varepsilon\widetilde{\boldsymbol{q}}^T\boldsymbol{u},\end{aligned} \tag{13b}$$

here $\widetilde{\boldsymbol{P}} = \widehat{\boldsymbol{P}} - \boldsymbol{P}$ has been used.

By applying Property 2 and adaptation law (8), we get

$$\frac{1}{2}\boldsymbol{x}^T\dot{\boldsymbol{M}}(\boldsymbol{q})\boldsymbol{x} = \boldsymbol{x}^T\boldsymbol{C}(\boldsymbol{q},\dot{\boldsymbol{q}})\boldsymbol{x}, \tag{14a}$$

$$\varepsilon\boldsymbol{x}^T\dot{\boldsymbol{M}}(\boldsymbol{q})\widetilde{\boldsymbol{q}} = \varepsilon\boldsymbol{x}^T\boldsymbol{C}(\boldsymbol{q},\dot{\boldsymbol{q}})\widetilde{\boldsymbol{q}} + \varepsilon\boldsymbol{x}^T\boldsymbol{C}^T(\boldsymbol{q},\dot{\boldsymbol{q}})\widetilde{\boldsymbol{q}}, \tag{14b}$$

$$\widetilde{\boldsymbol{P}}^T\boldsymbol{\Phi}^{-1}\dot{\widetilde{\boldsymbol{P}}} = \widetilde{\boldsymbol{P}}^T\boldsymbol{\Phi}^{-1}\left[-\boldsymbol{\Phi}\boldsymbol{\Psi}^T\left(\boldsymbol{q},\dot{\boldsymbol{q}},\dot{\boldsymbol{q}}_r,\ddot{\boldsymbol{q}}_r\right)(\boldsymbol{x} + \varepsilon\widetilde{\boldsymbol{q}})\right] = -\left(\boldsymbol{x}^T + \varepsilon\widetilde{\boldsymbol{q}}^T\right)\boldsymbol{\Psi}\left(\boldsymbol{q},\dot{\boldsymbol{q}},\dot{\boldsymbol{q}}_r,\ddot{\boldsymbol{q}}_r\right)\widetilde{\boldsymbol{P}}, \tag{14c}$$

here $\dot{\widetilde{\boldsymbol{P}}} = \dot{\widehat{\boldsymbol{P}}}$ has been used.

Substituting (13) and (14) into (12) yields

$$\begin{aligned}\dot{V} = {} & -\boldsymbol{x}^T\boldsymbol{K}_P\widetilde{\boldsymbol{q}} - \boldsymbol{x}^T\boldsymbol{K}_D\dot{\widetilde{\boldsymbol{q}}} - \left(\boldsymbol{x}^T + \varepsilon\widetilde{\boldsymbol{q}}^T\right)\boldsymbol{K}_I\int_0^t\widetilde{\boldsymbol{q}}dl + \left(\boldsymbol{x}^T + \varepsilon\widetilde{\boldsymbol{q}}^T\right)\boldsymbol{\Lambda} \\ & - \left(\boldsymbol{x}^T + \varepsilon\widetilde{\boldsymbol{q}}^T\right)\boldsymbol{u} - \varepsilon\widetilde{\boldsymbol{q}}^T\boldsymbol{K}_P\widetilde{\boldsymbol{q}} + \dot{\varepsilon}\boldsymbol{x}^T\boldsymbol{M}(\boldsymbol{q})\widetilde{\boldsymbol{q}} + \varepsilon\boldsymbol{x}^T\boldsymbol{C}(\boldsymbol{q},\dot{\boldsymbol{q}})\widetilde{\boldsymbol{q}} \\ & + \varepsilon\boldsymbol{x}^T\boldsymbol{M}(\boldsymbol{q})\dot{\widetilde{\boldsymbol{q}}} + \widetilde{\boldsymbol{q}}^T\boldsymbol{K}_P\dot{\widetilde{\boldsymbol{q}}} + \gamma\widetilde{\boldsymbol{q}}^T\boldsymbol{K}_D\dot{\widetilde{\boldsymbol{q}}} + \frac{1}{2}\dot{\varepsilon}\widetilde{\boldsymbol{q}}^T\boldsymbol{K}_D\widetilde{\boldsymbol{q}}.\end{aligned} \tag{15}$$

Because $\boldsymbol{x}^T = \dot{\widetilde{\boldsymbol{q}}}^T + \gamma\widetilde{\boldsymbol{q}}^T$ and $\dot{\varepsilon} = -\gamma\varepsilon$, we obtain

$$-\boldsymbol{x}^T\boldsymbol{K}_P\widetilde{\boldsymbol{q}} = -\dot{\widetilde{\boldsymbol{q}}}^T\boldsymbol{K}_P\widetilde{\boldsymbol{q}} - \gamma\widetilde{\boldsymbol{q}}^T\boldsymbol{K}_P\widetilde{\boldsymbol{q}}, \tag{16a}$$

$$-\boldsymbol{x}^T\boldsymbol{K}_D\dot{\widetilde{\boldsymbol{q}}} = -\dot{\widetilde{\boldsymbol{q}}}^T\boldsymbol{K}_D\dot{\widetilde{\boldsymbol{q}}} - \gamma\widetilde{\boldsymbol{q}}^T\boldsymbol{K}_D\dot{\widetilde{\boldsymbol{q}}}, \tag{16b}$$

$$\dot{\varepsilon}\boldsymbol{x}^T\boldsymbol{M}(\boldsymbol{q})\widetilde{\boldsymbol{q}} = -\gamma\varepsilon\dot{\widetilde{\boldsymbol{q}}}^T\boldsymbol{M}(\boldsymbol{q})\widetilde{\boldsymbol{q}} - \gamma^2\varepsilon\widetilde{\boldsymbol{q}}^T\boldsymbol{M}(\boldsymbol{q})\widetilde{\boldsymbol{q}}, \tag{16c}$$

$$\varepsilon\boldsymbol{x}^T\boldsymbol{C}(\boldsymbol{q},\dot{\boldsymbol{q}})\widetilde{\boldsymbol{q}} = \varepsilon\dot{\widetilde{\boldsymbol{q}}}^T\boldsymbol{C}(\boldsymbol{q},\dot{\boldsymbol{q}})\widetilde{\boldsymbol{q}} + \varepsilon\gamma\widetilde{\boldsymbol{q}}^T\boldsymbol{C}(\boldsymbol{q},\dot{\boldsymbol{q}})\widetilde{\boldsymbol{q}}, \tag{16d}$$

$$\varepsilon\boldsymbol{x}^T\boldsymbol{M}(\boldsymbol{q})\dot{\widetilde{\boldsymbol{q}}} = \varepsilon\dot{\widetilde{\boldsymbol{q}}}^T\boldsymbol{M}(\boldsymbol{q})\dot{\widetilde{\boldsymbol{q}}} + \varepsilon\gamma\widetilde{\boldsymbol{q}}^T\boldsymbol{M}(\boldsymbol{q})\dot{\widetilde{\boldsymbol{q}}}, \tag{16e}$$

$$\frac{1}{2}\dot{\varepsilon}\widetilde{\boldsymbol{q}}^T\boldsymbol{K}_D\widetilde{\boldsymbol{q}} = -\frac{1}{2}\gamma\varepsilon\widetilde{\boldsymbol{q}}^T\boldsymbol{K}_D\widetilde{\boldsymbol{q}}. \tag{16f}$$

Using (16) in (15) leads to

$$\begin{aligned}\dot{V} = &-(\gamma+\varepsilon)\widetilde{\boldsymbol{q}}^T\boldsymbol{K}_P\widetilde{\boldsymbol{q}} - \dot{\widetilde{\boldsymbol{q}}}^T\boldsymbol{K}_D\dot{\widetilde{\boldsymbol{q}}} - \frac{1}{2}\gamma\varepsilon\widetilde{\boldsymbol{q}}^T\boldsymbol{K}_D\widetilde{\boldsymbol{q}} - \gamma^2\varepsilon\widetilde{\boldsymbol{q}}^T\boldsymbol{M}(\boldsymbol{q})\widetilde{\boldsymbol{q}}\\ &+ \varepsilon\dot{\widetilde{\boldsymbol{q}}}^T\boldsymbol{M}(\boldsymbol{q})\dot{\widetilde{\boldsymbol{q}}} + \varepsilon\dot{\widetilde{\boldsymbol{q}}}^T\boldsymbol{C}(\boldsymbol{q},\dot{\boldsymbol{q}})\widetilde{\boldsymbol{q}} + \gamma\varepsilon\widetilde{\boldsymbol{q}}^T\boldsymbol{C}(\boldsymbol{q},\dot{\boldsymbol{q}})\widetilde{\boldsymbol{q}}\\ &+ \left(\boldsymbol{x}^T + \varepsilon\widetilde{\boldsymbol{q}}^T\right)\left(\boldsymbol{\Lambda} - \boldsymbol{u} - \boldsymbol{K}_I\int_0^t\widetilde{\boldsymbol{q}}dl\right).\end{aligned} \tag{17}$$

Note that the following inequalities hold:

$$-(\gamma+\varepsilon)\widetilde{\boldsymbol{q}}^T\boldsymbol{K}_P\widetilde{\boldsymbol{q}} \le -(\gamma+\varepsilon)\lambda_{\min}(\boldsymbol{K}_P)\,\|\widetilde{\boldsymbol{q}}\|^2, \tag{18a}$$

$$-\dot{\widetilde{\boldsymbol{q}}}^T\boldsymbol{K}_D\dot{\widetilde{\boldsymbol{q}}} \le -\lambda_{\min}(\boldsymbol{K}_D)\,\|\dot{\widetilde{\boldsymbol{q}}}\|^2, \tag{18b}$$

$$-\frac{1}{2}\gamma\varepsilon\widetilde{\boldsymbol{q}}^T\boldsymbol{K}_D\widetilde{\boldsymbol{q}} \le -\frac{1}{2}\gamma\varepsilon\lambda_{\min}(\boldsymbol{K}_D)\,\|\widetilde{\boldsymbol{q}}\|^2, \tag{18c}$$

$$-\gamma^2\varepsilon\widetilde{\boldsymbol{q}}^T\boldsymbol{M}(\boldsymbol{q})\widetilde{\boldsymbol{q}} \le -\gamma^2\varepsilon m_m\|\widetilde{\boldsymbol{q}}\|^2, \tag{18d}$$

$$\varepsilon\dot{\widetilde{\boldsymbol{q}}}^T\boldsymbol{M}(\boldsymbol{q})\dot{\widetilde{\boldsymbol{q}}} \le \varepsilon m_M\|\dot{\widetilde{\boldsymbol{q}}}\|^2, \tag{18e}$$

$$\varepsilon\dot{\widetilde{\boldsymbol{q}}}^T\boldsymbol{C}(\boldsymbol{q},\dot{\boldsymbol{q}})\widetilde{\boldsymbol{q}} \le \varepsilon k_c\|\dot{\widetilde{\boldsymbol{q}}}\|\|\widetilde{\boldsymbol{q}}\| \le \frac{1}{2}\varepsilon k_c\left(\|\dot{\widetilde{\boldsymbol{q}}}\|^2 + \|\widetilde{\boldsymbol{q}}\|^2\right), \tag{18f}$$

$$\gamma\varepsilon\widetilde{\boldsymbol{q}}^T\boldsymbol{C}(\boldsymbol{q},\dot{\boldsymbol{q}})\widetilde{\boldsymbol{q}} \le \gamma\varepsilon k_c\|\widetilde{\boldsymbol{q}}\|^2, \tag{18g}$$

here Properties 1 and 4 have been used.

From (18), $\dot{V}$ given in (17) can be bounded as

$$\begin{aligned}\dot{V} \le &-\left[(\gamma+\varepsilon)\lambda_{\min}(\boldsymbol{K}_P) + \frac{1}{2}\gamma\varepsilon\lambda_{\min}(\boldsymbol{K}_D)\right.\\ &\left. +\ \gamma^2\varepsilon m_m - \left(\frac{1}{2}+\gamma\right)\varepsilon k_c\right]\|\widetilde{\boldsymbol{q}}\|^2\\ &-\ \left[\lambda_{\min}(\boldsymbol{K}_D) - \varepsilon m_M - \frac{1}{2}\varepsilon k_c\right]\|\dot{\widetilde{\boldsymbol{q}}}\|^2\\ &+\ \left(\boldsymbol{x}^T + \varepsilon\widetilde{\boldsymbol{q}}^T\right)\boldsymbol{\Lambda} + \left\|\boldsymbol{x}^T + \varepsilon\widetilde{\boldsymbol{q}}^T\right\|\left(\|\boldsymbol{u}\| + \|\boldsymbol{K}_I\|\left\|\int_0^t\widetilde{\boldsymbol{q}}dl\right\|\right).\end{aligned} \tag{19}$$

From (9), we have

$$\left(\boldsymbol{x}^T+\varepsilon\tilde{\boldsymbol{q}}^T\right)\boldsymbol{\Lambda}=-\left[b_0+b_1\|\dot{\boldsymbol{q}}\|+b_2\|\boldsymbol{q}\|+\|\boldsymbol{K}_I\|\left\|\int_0^t\tilde{\boldsymbol{q}}dl\right\|\right]\times\sum_{i=1}^n|x_i+\varepsilon\tilde{q}_i|$$
$$\leq-\left(\|\boldsymbol{u}\|+\|\boldsymbol{K}_I\|\left\|\int_0^t\tilde{\boldsymbol{q}}dl\right\|\right)\sum_{i=1}^n|x_i+\varepsilon\tilde{q}_i|$$
$$\leq-\left\|\boldsymbol{x}^T+\varepsilon\tilde{\boldsymbol{q}}^T\right\|\left(\|\boldsymbol{u}\|+\|\boldsymbol{K}_I\|\left\|\int_0^t\tilde{\boldsymbol{q}}dl\right\|\right), \tag{20}$$

here Assumption 2 has been used.

Thus, using (20) in (19), we obtain

$$\dot{V}\leq-\left[(\gamma+\varepsilon)\lambda_{\min}(\boldsymbol{K}_P)+\frac{1}{2}\gamma\varepsilon\lambda_{\min}(\boldsymbol{K}_D)+\gamma^2\varepsilon m_m-\left(\frac{1}{2}+\gamma\right)\varepsilon k_c\right]\|\tilde{\boldsymbol{q}}\|^2-\left[\lambda_{\min}(\boldsymbol{K}_D)-\varepsilon m_M-\frac{1}{2}\varepsilon k_c\right]\|\dot{\tilde{\boldsymbol{q}}}\|^2. \tag{21}$$

From above, we know that $\dot{V}$ is nonpositive if the following conditions are satisfied:

$$\begin{cases}\lambda_{\min}(\boldsymbol{K}_F)/m_M>\varepsilon^2, \quad \boldsymbol{K}_F=(\gamma+\varepsilon)\boldsymbol{K}_D+\boldsymbol{K}_P,\\ (\gamma+\varepsilon)\lambda_{\min}(\boldsymbol{K}_P)+\frac{1}{2}\gamma\varepsilon\lambda_{\min}(\boldsymbol{K}_D)+\gamma^2\varepsilon m_m-\left(\frac{1}{2}+\gamma\right)\varepsilon k_c>0,\\ \lambda_{\min}(\boldsymbol{K}_D)-\varepsilon m_M-\frac{1}{2}\varepsilon k_c>0.\end{cases} \tag{22}$$

In fact, from the definition of ε given in (8) we can see that, with suitable choice of γ (e.g., $\gamma\geq 1$), ε will quickly exponentially converge to zero, which leads to that the terms containing ε in (22) fast approach to zero. Therefore, as time increase, the conditions (22) can always be satisfied. Thus V is eventually bounded, which in turn implies that $\tilde{\boldsymbol{q}}$, $\dot{\tilde{\boldsymbol{q}}}$, and $\tilde{\boldsymbol{P}}$ are eventually bounded vectors. Moreover, $\dot{V}$ is negative semidefinite and vanishes if and only if $\tilde{\boldsymbol{q}}=\boldsymbol{0}$ and $\dot{\tilde{\boldsymbol{q}}}=\boldsymbol{0}$. By invoking Lyapunov stability theory, we can conclude that $\tilde{\boldsymbol{q}}$ and $\dot{\tilde{\boldsymbol{q}}}$ eventually asymptotically converge to zero. On the other hand, due to that Property 4 is established on the premise that $\dot{\boldsymbol{q}}$ is bounded, $\tilde{\boldsymbol{q}}$ and $\dot{\tilde{\boldsymbol{q}}}$ are locally stable. This completes the proof. ∎

Remark 1. Theorem 1 implies that, for the robotic manipulator systems (1), when the upper bound of the uncertainties is known, the controller given in (7)–(9) guarantees the eventual local stability of the closed-loop system and zero steady-state errors for joint positions and velocities without the requirement of any equality/inequality constraints on the controller gains.

3.2 | Controller design with unknown upper bound of the uncertainties

For the robotic manipulator systems (1), when the upper bound of the uncertainties $\boldsymbol{u}$ is unknown, then consider the controller (7) with parameter adaptation law (8) and the following compensation terms:

$$\boldsymbol{\Lambda}=-\frac{(\hat{b}\theta)^2}{\hat{b}\theta\|\boldsymbol{x}+\varepsilon\tilde{\boldsymbol{q}}\|+\omega^2}(\boldsymbol{x}+\varepsilon\tilde{\boldsymbol{q}}), \tag{23}$$

$$\dot{\hat{b}}=\lambda_1\theta\|\boldsymbol{x}+\varepsilon\tilde{\boldsymbol{q}}\|, \quad \hat{b}(0)=0, \tag{24}$$

$$\dot{\omega}=-\lambda_2\omega, \quad \omega(0)\neq 0, \tag{25}$$

where $\hat{b}$ is the estimate of b and b is defined as $b = b_0 + b_1 + b_2 + \|\boldsymbol{K}_I\|$, θ is defined as $\theta = \max\left(1, \|\dot{\boldsymbol{q}}\|, \|\boldsymbol{q}\|, \left\|\int_0^t \tilde{\boldsymbol{q}} dl\right\|\right)$, and λ_1, λ_2 are positive constants.

Theorem 2. Given the robotic manipulator dynamics (1) with unknown upper bound of the uncertainties $\boldsymbol{u}$ controlled by the controller (7), (8), and (23)–(25), the position and velocity tracking errors $\tilde{\boldsymbol{q}}$ and $\dot{\tilde{\boldsymbol{q}}}$ eventually asymptotically converge to zero locally, and the parameter estimation error $\tilde{\boldsymbol{P}}$ as defined in Section 3.1 is eventually bounded.

Proof. Consider the Lyapunov candidate function as follows:

$$V = \frac{1}{2}\boldsymbol{\eta}^T \boldsymbol{H}\boldsymbol{\eta} + \frac{1}{2}\tilde{\boldsymbol{P}}^T \boldsymbol{\Phi}^{-1}\tilde{\boldsymbol{P}} + \frac{1}{2}\lambda_1^{-1}\tilde{b}^2 + \frac{1}{2}\lambda_2^{-1}\omega^2, \tag{26}$$

where $\boldsymbol{\eta}$, $\boldsymbol{H}$ are defined in Section 3.1, and $\tilde{b} = b - \hat{b}$.

As mentioned in Section 3.1, if the first inequality condition in (22) is satisfied, then the matrix $\boldsymbol{H}$ is symmetric positive definite and consequently $V > 0$.

Differentiating V with respect to time and from (17), we get

$$\begin{aligned}
\dot{V} = & -(\gamma + \varepsilon)\tilde{\boldsymbol{q}}^T \boldsymbol{K}_P \tilde{\boldsymbol{q}} - \dot{\tilde{\boldsymbol{q}}}^T \boldsymbol{K}_D \dot{\tilde{\boldsymbol{q}}} - \frac{1}{2}\gamma\varepsilon\tilde{\boldsymbol{q}}^T \boldsymbol{K}_D \tilde{\boldsymbol{q}} - \gamma^2\varepsilon\tilde{\boldsymbol{q}}^T \boldsymbol{M}(\boldsymbol{q})\tilde{\boldsymbol{q}} \\
& + \varepsilon\dot{\tilde{\boldsymbol{q}}}^T \boldsymbol{M}(\boldsymbol{q})\dot{\tilde{\boldsymbol{q}}} + \varepsilon\dot{\tilde{\boldsymbol{q}}}^T \boldsymbol{C}(\boldsymbol{q}, \dot{\boldsymbol{q}})\tilde{\boldsymbol{q}} + \gamma\varepsilon\tilde{\boldsymbol{q}}^T \boldsymbol{C}(\boldsymbol{q}, \dot{\boldsymbol{q}})\tilde{\boldsymbol{q}} \\
& + \left(\boldsymbol{x}^T + \varepsilon\tilde{\boldsymbol{q}}^T\right)\left(\boldsymbol{\Lambda} - \boldsymbol{u} - \boldsymbol{K}_I \int_0^t \tilde{\boldsymbol{q}} dl\right) + \lambda_1^{-1}\tilde{b}\dot{\tilde{b}} + \lambda_2^{-1}\omega\dot{\omega}.
\end{aligned} \tag{27}$$

Note that

$$\begin{aligned}
& -\left(\boldsymbol{x}^T + \varepsilon\tilde{\boldsymbol{q}}^T\right)\left(\boldsymbol{u} + \boldsymbol{K}_I \int_0^t \tilde{\boldsymbol{q}} dl\right) \\
& \leq \left\|\boldsymbol{x}^T + \varepsilon\tilde{\boldsymbol{q}}^T\right\| \left(\|\boldsymbol{u}\| + \|\boldsymbol{K}_I\| \left\|\int_0^t \tilde{\boldsymbol{q}} dl\right\|\right) \\
& \leq \left\|\boldsymbol{x}^T + \varepsilon\tilde{\boldsymbol{q}}^T\right\| \left[b_0 + b_1\|\dot{\boldsymbol{q}}\| + b_2\|\boldsymbol{q}\| + \|\boldsymbol{K}_I\| \left\|\int_0^t \tilde{\boldsymbol{q}} dl\right\|\right] \\
& \leq \|\boldsymbol{x} + \varepsilon\tilde{\boldsymbol{q}}\| b\theta,
\end{aligned} \tag{28}$$

here Assumption 2 and the definitions of b and θ have been used.

With $\dot{\tilde{b}} = -\dot{\hat{b}}$, (23)–(25) and (28), we have

$$\begin{aligned}
& \left(\boldsymbol{x}^T + \varepsilon\tilde{\boldsymbol{q}}^T\right)\left(\boldsymbol{\Lambda} - \boldsymbol{u} - \boldsymbol{K}_I \int_0^t \tilde{\boldsymbol{q}} dl\right) + \lambda_1^{-1}\tilde{b}\dot{\tilde{b}} + \lambda_2^{-1}\omega\dot{\omega} \\
& \leq -\frac{(\hat{b}\theta)^2}{\hat{b}\theta\|\boldsymbol{x} + \varepsilon\tilde{\boldsymbol{q}}\| + \omega^2}\|\boldsymbol{x} + \varepsilon\tilde{\boldsymbol{q}}\|^2 + b\theta\|\boldsymbol{x} + \varepsilon\tilde{\boldsymbol{q}}\| - \tilde{b}\theta\|\boldsymbol{x} + \varepsilon\tilde{\boldsymbol{q}}\| - \omega^2 \\
& = -\frac{\omega^4}{\hat{b}\theta\|\boldsymbol{x} + \varepsilon\tilde{\boldsymbol{q}}\| + \omega^2} \leq 0.
\end{aligned} \tag{29}$$

Then, from (29) and (18), $\dot{V}$ given in (27) can be bounded as (21). Now, the stability conditions of Theorem 2 are the same as that of Theorem 1. Thus, the same stability results on $\tilde{\boldsymbol{q}}$, $\dot{\tilde{\boldsymbol{q}}}$, and $\tilde{\boldsymbol{P}}$ are obtained as in Theorem 1. Then Theorem 2 is proved. ■

Remark 2. Theorem 2 implies that, for the robotic manipulator systems (1), when the upper bound of the uncertainties is unknown, the controller given in (7), (8), and (23)–(25) guarantees the eventual local stability of the closed-loop system and zero steady-state errors for joint positions and velocities without the requirement of any equality/inequality constraints on the controller gains.

Remark 3. Although the eventual local stability of the closed-loop system and zero steady-state errors for joint positions and velocities are guaranteed under the two proposed controllers with no dependent on the conditions (22), big system overshoots may occur in the transient process if the conditions (22) are seriously unsatisfied in the initial stage. Such undesired big system overshoots can be avoided by making the conditions (22) satisfied at the initial time $t = 0$ s, that is, making the following conditions satisfied:

$$\begin{cases} \lambda_{\min}\left(\boldsymbol{K}_{F0}\right)/m_M > \lambda^2, \;\; \boldsymbol{K}_{F0} = (\gamma+\lambda)\boldsymbol{K}_D + \boldsymbol{K}_P, \\ (\gamma+\lambda)\lambda_{\min}\left(\boldsymbol{K}_P\right) + \frac{\gamma\lambda}{2}\lambda_{\min}\left(\boldsymbol{K}_D\right) + \gamma^2\lambda m_m - \left(\frac{1}{2}+\gamma\right)\lambda k_c > 0, \\ \lambda_{\min}\left(\boldsymbol{K}_D\right) - \lambda\left(m_M + \frac{1}{2}k_c\right) > 0. \end{cases} \tag{30}$$

Remark 4. Equation (30) implies that the parameter λ will considerably influence the system overshoots at the initial stage. If λ is chosen a large value such that the conditions (30) are not satisfied, big system overshoots may occur at the initial stage. Moreover, the larger the value of λ, the bigger the system overshoots.

Remark 5. Compared with the classical PID controller and the adaptive PID controllers presented in Reference 13, the two proposed adaptive PID controllers guarantee the eventual stability of the closed-loop system without the need of any equality/inequality constraints on the controller gains. Moreover, in contrast to the adaptive PID controller presented in Reference 12, the two proposed adaptive PID controllers guarantee the convergence of the joint position and velocity tracking errors to zero instead of H_∞ tracking performance.

Remark 6. Note that the two adaptive PID controllers proposed in this study require the information of the dynamic model parameters. Some recent work on adaptive neural and adaptive fuzzy control of robot manipulators can avoid the requirement of such information. Interested readers can refer to References 34 and 35.

3.3 | Some guidance for controller parameters selection

The tracking performance largely depends on the parameters of the two designed controllers. Here are some guidance of selecting these parameters and the effects of them in the system.

1. The PID parameters, that is, $\boldsymbol{K}_P$, $\boldsymbol{K}_D$, and $\boldsymbol{K}_I$ can be selected by trial and error. The basic principle is as follows: The proportional gain $\boldsymbol{K}_P$ should be chosen appropriately large to improve the response speed and the steady-state accuracy of the system, and suppress the influence of the uncertainties on the steady state of the system, but it cannot be chosen too large since excessive proportional gain can easily lead to system overshoot and oscillation, and may make the system unstable; The integral gain $\boldsymbol{K}_I$ is used to eliminate the steady-state errors, it is not advisable to be chosen too large since if the integral action is too strong and the integral output changes too fast, it will cause the phenomenon of over-integration, resulting in integral overshoot and oscillation; The differential gain $\boldsymbol{K}_D$ mainly affects the dynamic quality of the control system. Appropriate differential action can speed up the system response, effectively reduce overshoot, improve the dynamic characteristics of the system, and increase the stability of the system. It is suggested that the differential gain should be chosen relatively small since too strong differential action will also cause the system to be unstable and cause oscillation.
2. The gain $\boldsymbol{\Phi}$ determines the estimated speed of the unknown manipulator and load parameter $\boldsymbol{P}$, the elements in $\boldsymbol{\Phi}$ are suggested to be chosen greater or equal to 1 so as to guarantee a fast estimated speed. But they cannot be chosen too large to avoid over-estimation.
3. The parameter γ in the exponential convergent factor ε should be chosen such that $\gamma \geq 1$ to make ε quickly converge so as to make the conditions (22) quickly be satisfied, and consequently the stability of the closed-loop system can be quickly guaranteed. The parameter λ is suggested to be chosen small to make the conditions (30) be satisfied so as to avoid big system overshoots at the initial stage, the details about how the parameter λ influences the system overshoots at the initial stage can refer to Remark 4.
4. The parameter λ_1 in the adaptation law (24) should be chosen large to ensure a fast estimation of the bound information of the uncertainties so as to provide an effective compensation for the uncertainties. But the parameter λ_2 should be chosen small since large λ_2 will lead to fast decrease of the parameter ω, and consequently results in the control inputs chattering according to the control law (23).

4 | SIMULATION RESULTS AND DISCUSSION

In this section, simulation studies are performed to demonstrate the two proposed adaptive PID controllers. A two-link planar rigid manipulator (see Figure 1) taken from Reference 32 with masses m_1, m_2 (including unknown load), lengths l_1, l_2, angles q_1, q_2, and torques τ_1, τ_2 are used for simulations. The dynamic model of the manipulator is described by (1) with

$$\boldsymbol{M}(\boldsymbol{q}) = \begin{bmatrix} (m_1+m_2)\,l_1^2 + m_2 l_2^2 + 2m_2 l_1 l_2 c_2 & m_2 l_2^2 + m_2 l_1 l_2 c_2 \\ m_2 l_2^2 + m_2 l_1 l_2 c_2 & m_2 l_2^2 \end{bmatrix}, \tag{31}$$

$$\boldsymbol{C}(\boldsymbol{q}, \dot{\boldsymbol{q}}) = \begin{bmatrix} -m_2 l_1 l_2 \dot{q}_2 s_2 & -m_2 l_1 l_2 \left(\dot{q}_1 + \dot{q}_2\right) s_2 \\ m_2 l_1 l_2 \dot{q}_1 s_2 & 0 \end{bmatrix}, \tag{32}$$

$$\boldsymbol{G}(\boldsymbol{q}) = \begin{bmatrix} (m_1+m_2)\,l_1 g c_2 + m_2 l_2 g c_{12} \\ m_2 l_2 g c_{12} \end{bmatrix}, \tag{33}$$

in which $c_2 = \cos(q_2)$, $s_2 = \sin(q_2)$, $c_{12} = \cos(q_1+q_2)$, and g is the gravitational acceleration. The parameter values are taken from Reference 32 and are given by $m_1 = m_2 = 0.5$ kg, $l_1 = 1$m, $l_2 = 0.8$m. Thus we can take m_M in Property 1 as $m_M = 2.37$. Provided the upper bound of the joint velocities as $|\dot{q}_i| \le 3$ rad/s $(i = 1, 2)$, then we can take k_c in Property 4 as $k_c = 2.75$. Let the unknown manipulator and load parameters vector $\boldsymbol{P} = \left[p_1,\ \ p_2,\ \ p_3\right]^T$ be $p_1 = (m_1+m_2)\,l_1^2$, $p_2 = m_2 l_2^2$, $p_3 = m_2 l_1 l_2$ such as in Reference 32, then the regression matrix $\boldsymbol{\Psi}\left(\boldsymbol{q}, \dot{\boldsymbol{q}}, \dot{\boldsymbol{q}}_r, \ddot{\boldsymbol{q}}_r\right) = \left(\psi_{ij}\right)_{2\times 3}$ defined in (5) can be obtained as $\psi_{11} = \ddot{q}_{r1} + e_1 c_2$, $\psi_{12} = \ddot{q}_{r1} + \ddot{q}_{r2}$, $\psi_{13} = 2\ddot{q}_{r1} c_2 + \ddot{q}_{r2} c_2 - \dot{q}_2 \dot{q}_{r1} s_2 - \left(\dot{q}_1 + \dot{q}_2\right)\dot{q}_{r2} s_2 + e_1 c_{12}$, $\psi_{21} = 0$, $\psi_{22} = \psi_{12}$, $\psi_{23} = \ddot{q}_{r1} c_2 + \dot{q}_1 \dot{q}_{r1} s_2 + e_1 c_{12}$ where $e_1 = g/l_1$.

The uncertainties are chosen as

$$\boldsymbol{u} = [3 \quad 4]^T + 3\dot{\boldsymbol{q}} + 5\boldsymbol{q} \ \ \text{Nm}. \tag{34}$$

The desired joint trajectory is selected as

$$q_{d1} = q_{d2} = \pi/2 + 0.3\pi[1 - \cos(1.26t)] \ \ \text{rad}. \tag{35}$$

The initial values of the joint positions and velocities are chosen as $q_1(0) = 4\pi/9$ rad, $q_2(0) = 7\pi/18$ rad, $\dot{q}_1(0) = \dot{q}_2(0) = 0$ rad/s. The initial values of the adaptive parameters $\hat{p}_i$ $(i = 1, 2, 3)$ in parameter adaptation law (8) are chosen as $\hat{p}_1(0) = 4.1$, $\hat{p}_2(0) = 0.1$, $\hat{p}_3(0) = 1.7$.

Here two simulation studies are carried out. The purpose of the first simulation study is to compare the two proposed adaptive PID controllers with the classical PID controller, the adaptive PD controller,[8] the LADRC,[28,29] and the NDOB[30] based adaptive PID controller in terms of control performances when the conditions (30) are satisfied. The purpose of the second simulation study is threefold: (1) to verify the property that the two proposed adaptive PID controllers guarantee the eventual local stability of the closed-loop system and zero steady-state errors for joint positions and velocities without the requirement of any equality/inequality constraints on the controller gains, namely, with no dependent

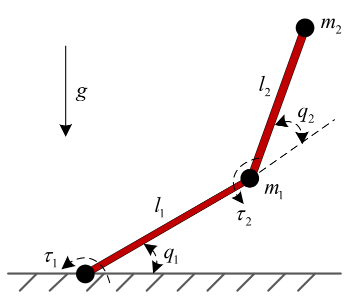

FIGURE 1 Two-link planar rigid robotic manipulator

on the conditions (22); (2) to investigate the influence of the parameter λ on the performances of the two proposed adaptive PID controllers; and (3) to compare the two proposed adaptive PID controllers with the classical PID controller, the adaptive PD controller,[8] the LADRC,[28,29] and the NDOB[30] based adaptive PID controller in terms of control performances when the conditions (30) are not satisfied.

4.1 | The first simulation study

The task is to force the robotic manipulator to track the desired trajectory described in (35). Two cases are considered: Case 1 with the known upper bound of the uncertainties and Case 2 with the unknown upper bound of the uncertainties. For each case, five controllers are implemented, namely, the classical PID controller, the adaptive PD controller,[8] the LADRC,[28,29] the NDOB[30] based adaptive PID controller, and the corresponding adaptive PID controller proposed in this work. The classical PID controller is described as

$$\boldsymbol{\tau} = -\boldsymbol{K}_P\tilde{\boldsymbol{q}} - \boldsymbol{K}_D\dot{\tilde{\boldsymbol{q}}} - \boldsymbol{K}_I\int_0^t \tilde{\boldsymbol{q}}dl. \tag{36}$$

The adaptive PD controller presented in Reference 8 is given by

$$\begin{aligned} \boldsymbol{\tau} &= \boldsymbol{\Psi}\left(\boldsymbol{q}, \dot{\boldsymbol{q}}, \dot{\boldsymbol{q}}_r, \ddot{\boldsymbol{q}}_r\right)\hat{\boldsymbol{P}} - \boldsymbol{K}_D\boldsymbol{x}, \\ \dot{\hat{\boldsymbol{P}}} &= -\boldsymbol{\Phi}\boldsymbol{\Psi}^T\left(\boldsymbol{q}, \dot{\boldsymbol{q}}, \dot{\boldsymbol{q}}_r, \ddot{\boldsymbol{q}}_r\right)\boldsymbol{x}. \end{aligned} \tag{37}$$

The LADRC is designed based on References 28 and 29, that is:

According to References 28 and 29, the linear extended state observer (LESO) of the robot system (1) is

$$\begin{cases} \dot{\hat{\boldsymbol{q}}} = \hat{\dot{\boldsymbol{q}}} + \boldsymbol{W}_1(\boldsymbol{q} - \hat{\boldsymbol{q}}), \\ \dot{\hat{\dot{\boldsymbol{q}}}} = \hat{\boldsymbol{F}} + \boldsymbol{B}\boldsymbol{\tau} + \boldsymbol{W}_2(\boldsymbol{q} - \hat{\boldsymbol{q}}) \quad \text{with} \quad \hat{\boldsymbol{q}}(0) = \boldsymbol{0}, \ \hat{\dot{\boldsymbol{q}}}(0) = \boldsymbol{0}, \ \hat{\boldsymbol{F}}(0) = \boldsymbol{0}, \\ \dot{\hat{\boldsymbol{F}}} = \boldsymbol{W}_3(\boldsymbol{q} - \hat{\boldsymbol{q}}), \end{cases} \tag{38}$$

where $\hat{\boldsymbol{q}}$ and $\hat{\dot{\boldsymbol{q}}}$ are the estimations of $\boldsymbol{q}$ and $\dot{\boldsymbol{q}}$, $\hat{\boldsymbol{F}}$ is the estimation of the total uncertainties $\boldsymbol{F}$, $\boldsymbol{F} = -\boldsymbol{M}^{-1}(\boldsymbol{q})(\boldsymbol{C}(\boldsymbol{q}, \dot{\boldsymbol{q}})\dot{\boldsymbol{q}} + \boldsymbol{G}(\boldsymbol{q}) + \boldsymbol{u} - \boldsymbol{\tau}) - \boldsymbol{B}\boldsymbol{\tau}$, $\boldsymbol{B}$ is defined as the control coefficient matrix, $\boldsymbol{W}_1$, $\boldsymbol{W}_2$, and $\boldsymbol{W}_3$ are the designed parameter matrices of the LESO, $\boldsymbol{W}_1 = diag\,(3\omega_{01},\ 3\omega_{02})$, $\boldsymbol{W}_2 = diag\left(3\omega_{01}^2,\ 3\omega_{02}^2\right)$, and $\boldsymbol{W}_3 = diag\left(\omega_{01}^3,\ \omega_{02}^3\right)$, ω_{01} and ω_{02} are the control bandwidths of the observer.

Then the control law is designed as

$$\boldsymbol{\tau} = \boldsymbol{B}^{-1}\left(-\hat{\boldsymbol{F}} - \boldsymbol{K}_P\tilde{\boldsymbol{q}} - \boldsymbol{K}_D\dot{\tilde{\boldsymbol{q}}}\right). \tag{39}$$

The NDOB based adaptive PID controller is designed based on the NDOB presented in Reference 30, that is:

According to Reference 30, the NDOB of the robot system (1) is designed as

$$\begin{cases} \hat{\boldsymbol{u}} = \boldsymbol{z} + \boldsymbol{d}, \\ \dot{\boldsymbol{z}} = \boldsymbol{L}\boldsymbol{M}^{-1}(\boldsymbol{q})(\boldsymbol{z} + \boldsymbol{C}(\boldsymbol{q}, \dot{\boldsymbol{q}})\dot{\boldsymbol{q}} + \boldsymbol{G}(\boldsymbol{q}) + \boldsymbol{d} - \boldsymbol{\tau}) \quad \text{with} \quad \boldsymbol{z}(0) = \boldsymbol{0}, \\ \boldsymbol{d} = \int_0^t \boldsymbol{L}\ddot{\boldsymbol{q}}dl, \end{cases} \tag{40}$$

in which $\hat{\boldsymbol{u}}$ is the estimation of the uncertainties $\boldsymbol{u}$, $\boldsymbol{z}$ is an auxiliary variable vector, $\boldsymbol{d}$ is a designed function vector, and $\boldsymbol{L}$ is a designed parameter matrix of the NDOB.

Based on the above NDOB, the NDOB based adaptive PID controller can be described as

$$\boldsymbol{\tau} = -\boldsymbol{K}_P\tilde{\boldsymbol{q}} - \boldsymbol{K}_D\dot{\tilde{\boldsymbol{q}}} - \boldsymbol{K}_I\int_0^t \tilde{\boldsymbol{q}}dl + \boldsymbol{\Psi}\left(\boldsymbol{q}, \dot{\boldsymbol{q}}, \dot{\boldsymbol{q}}_r, \ddot{\boldsymbol{q}}_r\right)\hat{\boldsymbol{P}} + \hat{\boldsymbol{u}}. \tag{41}$$

TABLE 1 Controller parameters for the five controllers for both cases

PID	$\boldsymbol{K}_P = diag(90, 90)$, $\boldsymbol{K}_D = diag(15, 15)$, $\boldsymbol{K}_I = diag(50, 50)$
Adaptive PD	$\boldsymbol{K}_P = diag(90, 90)$, $\boldsymbol{K}_D = diag(15, 15)$, $\boldsymbol{\Phi} = diag(3, 1, 3)$, $\gamma = 6$
Adaptive PID	$\boldsymbol{K}_P = diag(90, 90)$, $\boldsymbol{K}_D = diag(15, 15)$, $\boldsymbol{K}_I = diag(50, 50)$, $\boldsymbol{\Phi} = diag(3, 1, 3)$, $\gamma = 6$, $\lambda = 0.1$
LADRC	$\boldsymbol{K}_P = diag(90, 90)$, $\boldsymbol{K}_D = diag(15, 15)$, $\omega_{01} = \omega_{02} = 15$, $\boldsymbol{B} = \begin{bmatrix} 1.4 & -0.1 \\ -0.1 & 1.4 \end{bmatrix}$
NDOB based adaptive PID (called DOB PID for short in simulation results)	$\boldsymbol{K}_P = diag(90, 90)$, $\boldsymbol{K}_D = diag(15, 15)$, $\boldsymbol{L} = diag(-150, -150)$

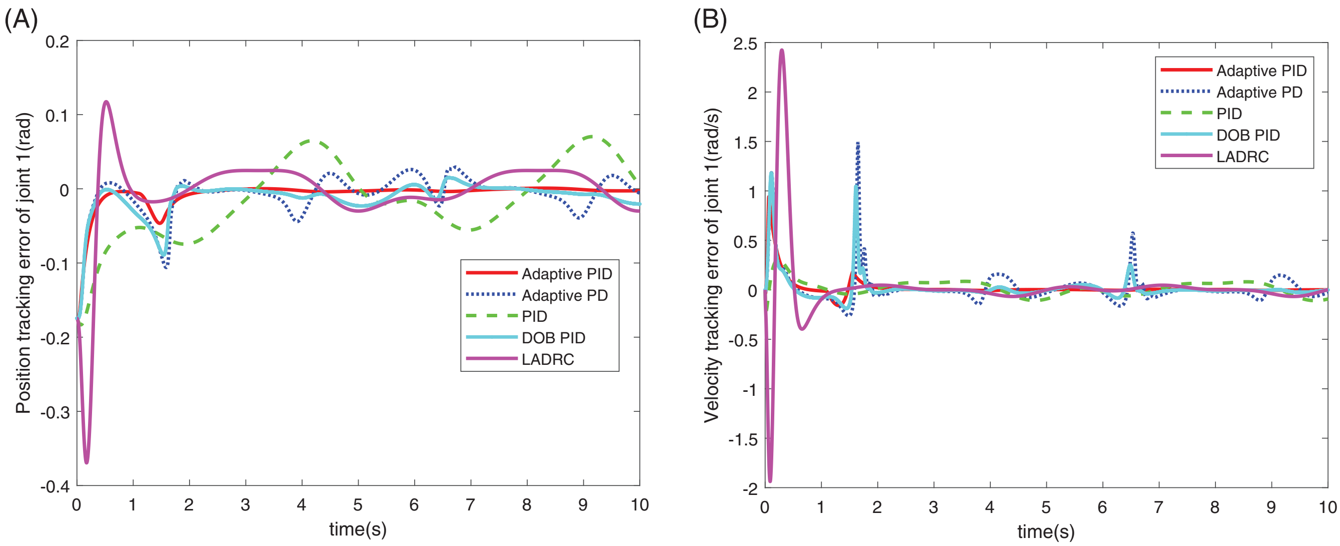

FIGURE 2 Position and velocity tracking errors of joint 1 for the five controllers in Case 1

In Case 1, for the proposed adaptive PID controller (7)–(9), the upper bound parameters of the uncertainties $\boldsymbol{u}$ can be selected as $b_0 = 5, b_1 = 3, b_2 = 5$. To eliminate the undesirable chattering due to the discontinuous sign function in (9), the saturation function $sat[(\boldsymbol{x} + \varepsilon\tilde{\boldsymbol{q}})/0.05] = \left(sat\left[\left(x_i + \varepsilon\tilde{q}_i\right)/0.05\right]\right)_{2\times1}$ is adopted to replace the sign function in (9), where

$$sat\left(\frac{x_i + \varepsilon\tilde{q}_i}{0.05}\right) = \begin{cases} \mathrm{sgn}\left(x_i + \varepsilon\tilde{q}_i\right), & \text{if} \left|\left(x_i + \varepsilon\tilde{q}_i\right)/0.05\right| \geq 1, \\ \left(x_i + \varepsilon\tilde{q}_i\right)/0.05, & \text{if} \left|\left(x_i + \varepsilon\tilde{q}_i\right)/0.05\right| < 1. \end{cases} \tag{42}$$

In Case 2, for the proposed adaptive PID controller (7), (8), and (23)–(25), θ is determined by $\theta = \max\left(1, \|\dot{\boldsymbol{q}}\|, \|\boldsymbol{q}\|, \left\|\int_0^t \tilde{\boldsymbol{q}} dl\right\|\right)$, λ_1, λ_2 are chosen as $\lambda_1 = 8$, $\lambda_2 = 0.4$, and the initial value of ω is selected as $\omega(0) = 100$.

To make the comparison fair and persuasive, for each case, the corresponding controller parameters for the five controllers are chosen exactly the same values as exhibited in Table 1. Note that the selected controller parameters can produce joint torques that are reasonable in practical engineering for each controller. Simulation results are shown in Figures 2–4 for Case 1 and in Figures 5–7 for Case 2.

The joint position and velocity tracking errors for the five controllers are illustrated in Figures 2 and 3 for Case 1 and are illustrated in Figures 5 and 6 for Case 2. It can be observed from these figures that for each case, all the five controllers can ensure the manipulator to track the desired joint trajectory. However, for each case, the proposed adaptive PID controllers perform the best in terms of tracking precision among the five controllers, showing better robustness against uncertainties than the other four controllers. The NDOB based adaptive PID controller (DOB PID) slightly outperforms the LADRC,

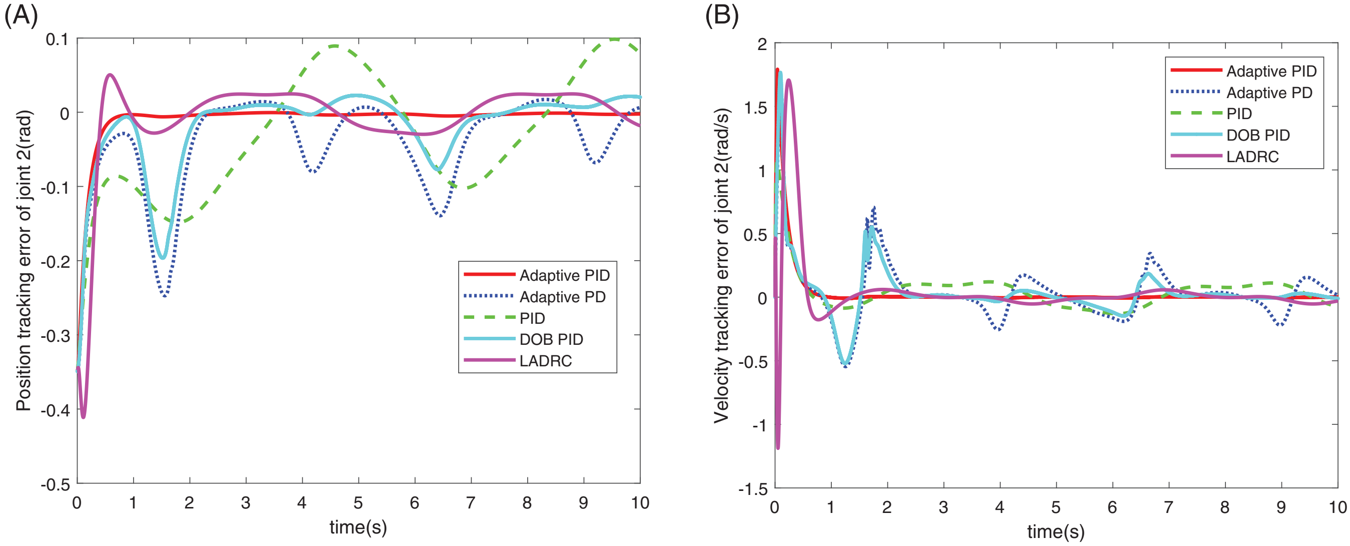

FIGURE 3 Position and velocity tracking errors of joint 2 for the five controllers in Case 1

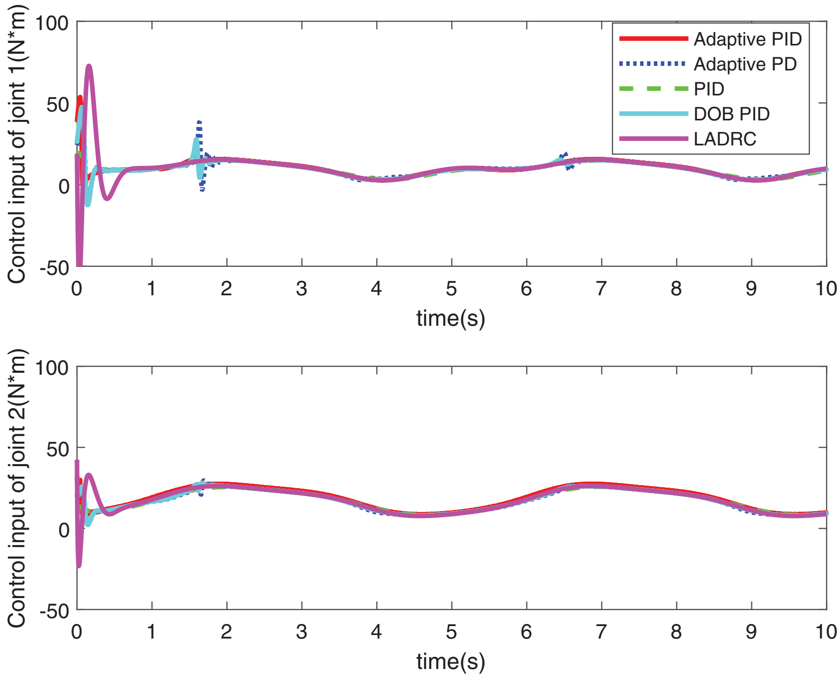

FIGURE 4 Control inputs for the five controllers in Case 1

this may because that the former only needs to estimate the uncertainties, but the later needs to estimate the whole robot dynamics, that is, the robot dynamic model plus the uncertainties. The adaptive PD and PID controllers perform the worst, since they do not contain the effective compensation term for the unmodeled dynamics and external disturbances. In addition, by comparing Figures 2 and 3 in Case 1 with Figures 5 and 6 in Case 2, it can be clearly seen that the proposed adaptive PID controller in Case 1 outperforms the proposed adaptive PID controller in Case 2, due to that in Case 1, the upper bound of the uncertainties is exactly known such that the proposed adaptive PID controller in this case can directly provide precise compensation for the uncertainties, but in Case 2, the upper bound of the uncertainties is not known, so the proposed adaptive PID controller in this case has to estimate the bound information of the uncertainties and the estimated errors exist, which effect the control performance. Apart from that, it can be observed that in Case 2, the performance of the DOB PID is closed to the proposed adaptive PID controllers, this is because that the two controllers have the same structure, only the way to estimate the uncertainties is different.

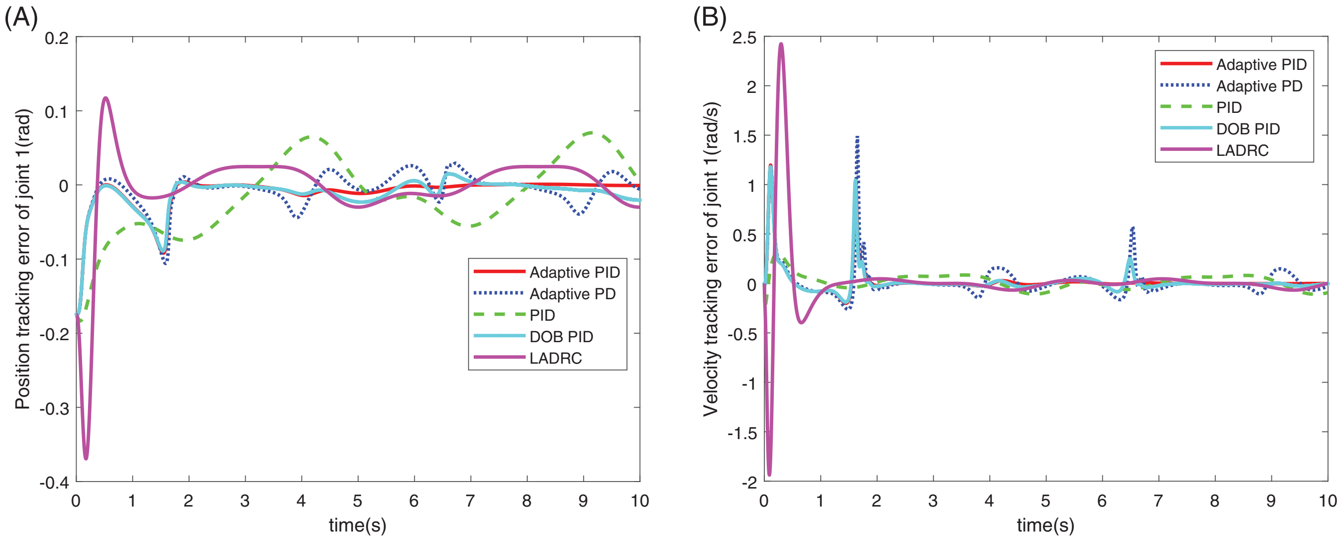

FIGURE 5 Position and velocity tracking errors of joint 1 for the five controllers in Case 2

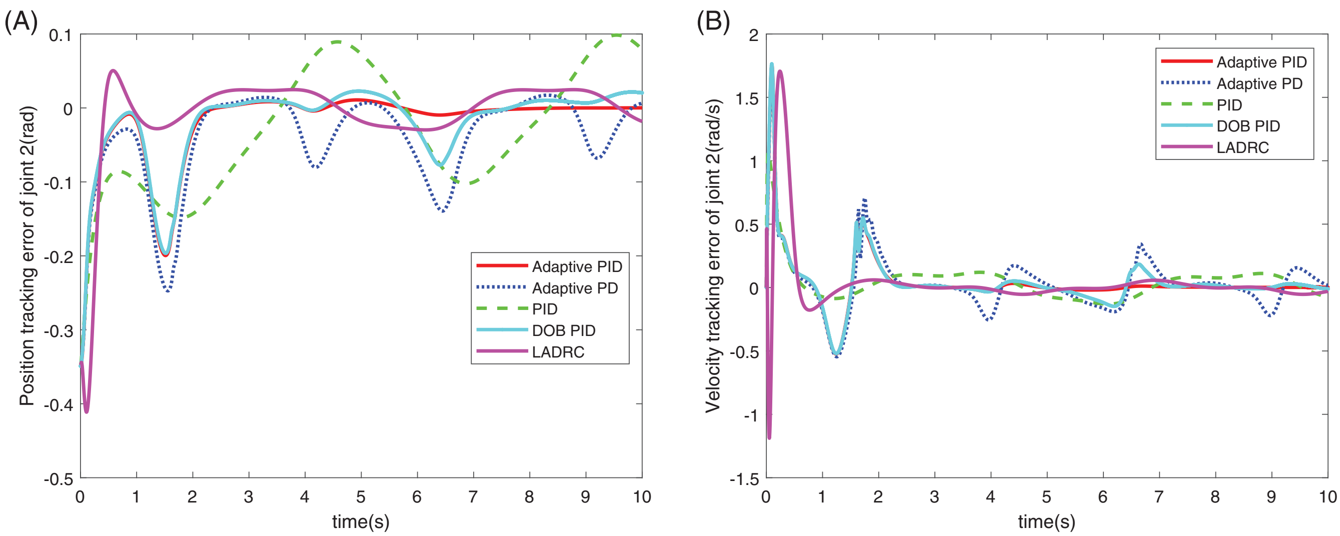

FIGURE 6 Position and velocity tracking errors of joint 2 for the five controllers in Case 2

The control inputs (i.e., the joint torques) for the five controllers are shown in Figure 4 for Case 1 and are shown in Figure 7 for Case 2. By observing the two figures, the control inputs for the five controllers during the steady state are almost the same, but the initial joint torques for the LADRC are a little bigger than for the other four controllers. As can be seen in Figure 4, the control input chattering is effectively weakened for the proposed adaptive PID controller in Case 1 due to using the saturation function. However, it is observed in Figure 7 that the control inputs have slight chattering after 9.5 s for the proposed adaptive PID controller in Case 2, this is because from the adaptation law of ω given in (25), ω will approach to zero as time increase, which leads to that $\boldsymbol{\Lambda}$ given in (23) tends to discontinuity near $(\tilde{\boldsymbol{q}}, \dot{\tilde{\boldsymbol{q}}}) = (\mathbf{0}, \mathbf{0})$, as a result, the control law $\boldsymbol{\tau}$ tends to discontinuity near $(\tilde{\boldsymbol{q}}, \dot{\tilde{\boldsymbol{q}}}) = (\mathbf{0}, \mathbf{0})$.

4.2 | The second simulation study

In this simulation study, the tracking task in the first simulation study is repeated. Also, two cases are considered: Case 1 with the known upper bound of the uncertainties and Case 2 with the unknown upper bound of the uncertainties. The

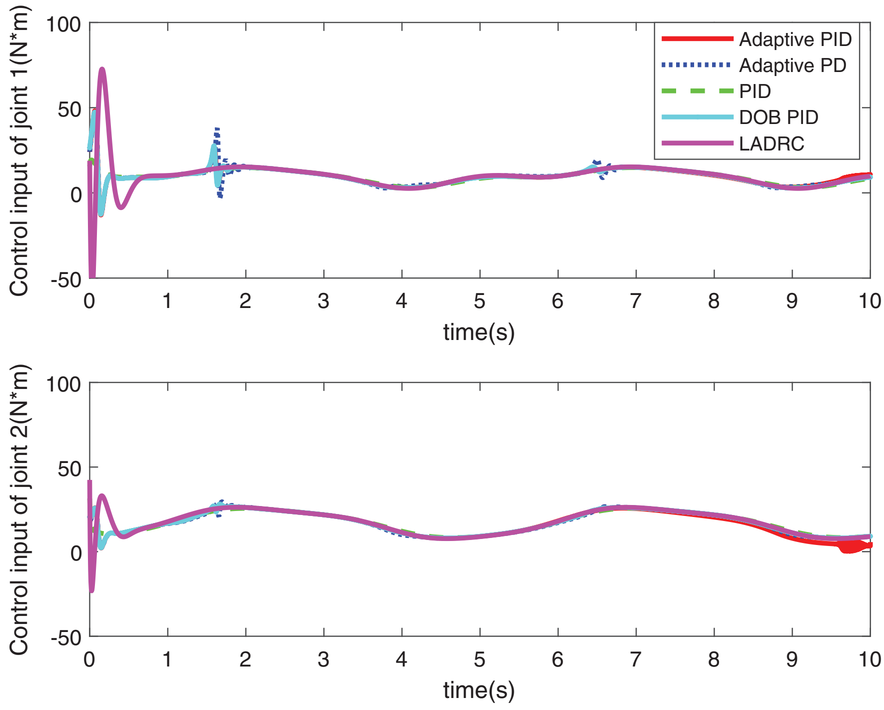

FIGURE 7 Control inputs for the five controllers in Case 2

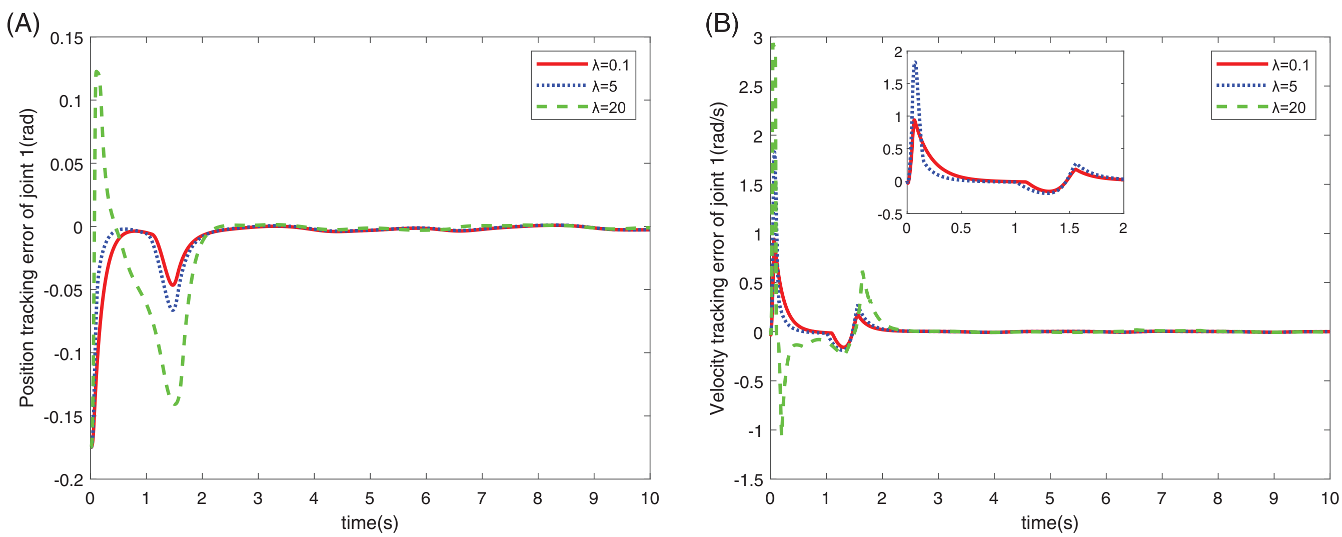

FIGURE 8 Position and velocity tracking errors of joint 1 for the proposed adaptive PID controller in Case 1 with three different values of λ

two proposed adaptive PID controllers are simulated with three different values of λ, namely, $\lambda = 0.1$, 5, and 20 where $\lambda = 0.1$ makes the conditions (30) satisfied while $\lambda = 5$ and 20 make the conditions (30) unsatisfied. Other controller parameters are the same as those in Table 1. Simulation results are shown in Figures 8 and 9 for Case 1 and are shown in Figures 10 and 11 for Case 2. Note that to keep the article reasonably concise, we only give out the position and velocity tracking results of the first joint for instance.

Figure 8 illustrates the position and velocity tracking errors of the first joint for the proposed adaptive PID controller in Case 1 with three different values of λ and Figure 9 illustrates those errors for the proposed adaptive PID controller in Case 2 with three different values of λ. It can be seen from the two figures that, even though the conditions (30) are not

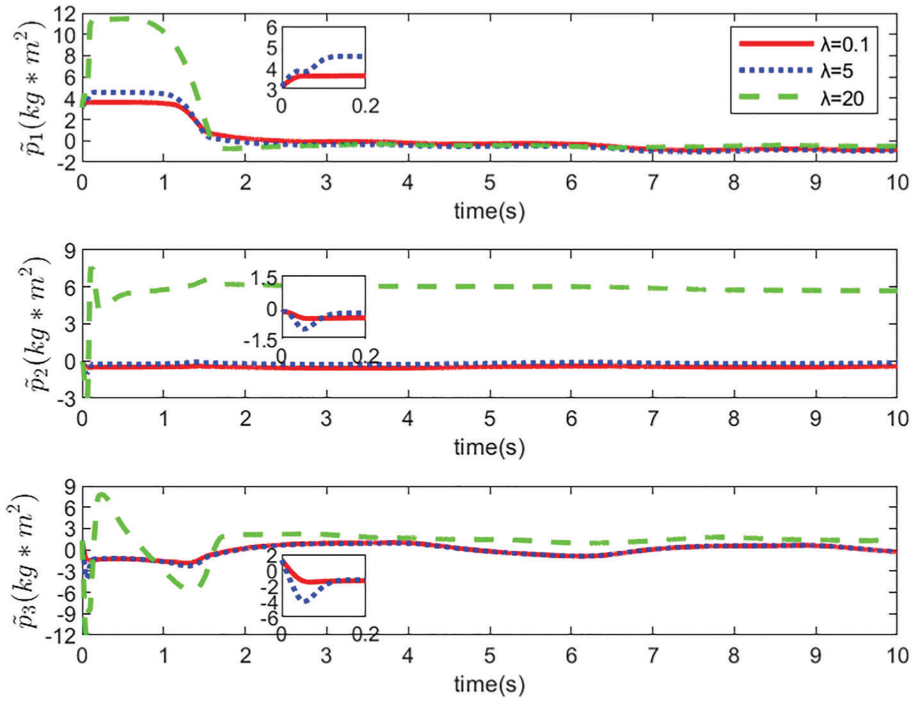

FIGURE 9 The parameter estimation error $\widetilde{\boldsymbol{P}}$ for the proposed adaptive PID controller in Case 1 with three different values of λ

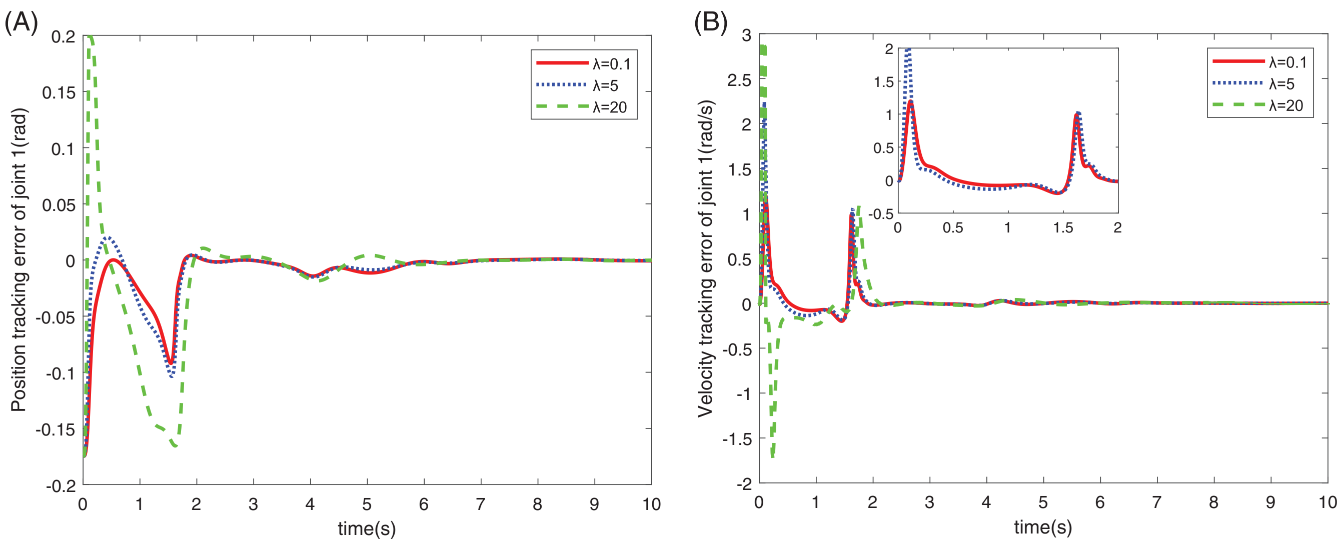

FIGURE 10 Position and velocity tracking errors of joint 1 for the proposed adaptive PID controller in Case 2 with three different values of λ

satisfied with $\lambda = 5$ and 20, the two proposed adaptive PID controllers still guarantee eventual asymptotical converge of the joint position and velocity tracking errors and the eventual boundedness of the parameter estimation error, which implies that the two proposed adaptive PID controllers ensure the eventual stability of the closed-loop system and zero steady-state errors for joint positions and velocities without the requirement of any equality/inequality constraints on the controller gains. However, the system overshoots are bigger for $\lambda = 5$ and 20 than for $\lambda = 0.1$. Moreover, the larger the value of λ, the bigger the system overshoots.

Figure 10 plots the estimation errors of the unknown manipulator and load parameters for the proposed adaptive PID controller in Case 1 with three different values of λ and Figure 11 plots those errors for the proposed adaptive PID

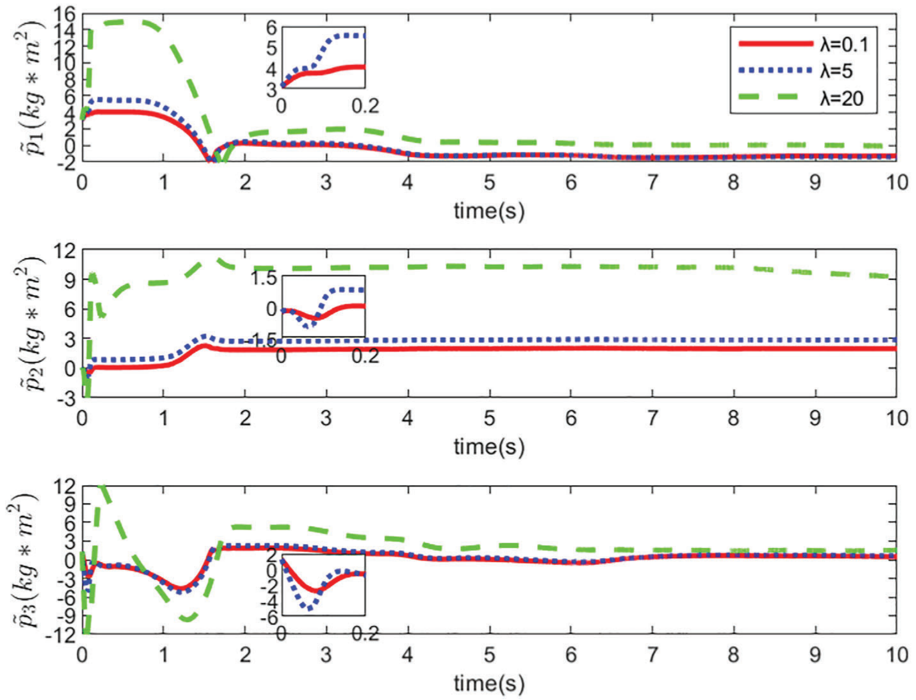

FIGURE 11 The parameter estimation error $\widetilde{\boldsymbol{P}}$ for the proposed adaptive PID controller in Case 2 with three different values of λ

controller in Case 2 with three different values of λ. Clearly, $\lambda = 0.1$ outperforms $\lambda = 5$ and 20 in terms of system overshoots and estimation precision and $\lambda = 20$ performs the worst.

In addition, by comparing Figures 8 and 10 with Figures 2 and 5, it can be observed that, even when the conditions (30) are not satisfied with $\lambda = 5$ and 20, the two proposed adaptive PID controllers can still provide smaller steady-state joint position and velocity tracking errors, namely, better robustness against uncertainties than the other four controllers. But the two proposed adaptive PID controllers obviously result in bigger system overshoots than the other four controllers when the conditions (30) are seriously unsatisfied with $\lambda = 20$. Therefore, it is concluded that, if the value of λ is not chosen too large such that the conditions (30) are not seriously unsatisfied, the two proposed adaptive PID controllers can still provide better overall control performances than the other four controllers.

5 | CONCLUSIONS

In this article, two novel adaptive PID controllers are proposed to solve the trajectory tracking control problem of robotic manipulators with known or unknown upper bound of the uncertainties, respectively. The two proposed adaptive PID controllers ensure the eventual local stability of the closed-loop system and zero steady-state errors for joint positions and velocities without the requirement of any equality/inequality constraints on the controller gains compared with the classical PID controller, the adaptive PID controllers presented in Reference 12, and the adaptive PID controller presented in Reference 13. Numerical simulations verify such feature of the two proposed adaptive PID controllers, and clarify the influence of the parameter λ on the performances of the two proposed adaptive PID controllers. In addition, the comparisons of the control performance between the two proposed adaptive PID controllers and the other four controllers, namely, the classical PID controller, the adaptive PD controller,[8] the LADRC,[28,29] and the NDOB[30] based adaptive PID controller have also been carried out through numerical simulations. The simulation results show that the two proposed adaptive PID controllers provide better robustness to uncertainties than the other four controllers.

ACKNOWLEDGMENTS

This work is supported by the National Natural Science Foundation of China under Grant 52101365, by the Shanghai Sailing Program under Grant 21YF1419800, by the Young Talent Project of China National Nuclear Corporation, by the State Key Laboratory of Ocean Engineering (Shanghai Jiao Tong University) under Grant GKZD010081, and by the LingChuang Research Project of China National Nuclear Corporation.

CONFLICT OF INTEREST

The authors declare no potential conflict of interests.

DATA AVAILABILITY STATEMENT

Data sharing is not applicable to this article as no datasets were generated or analyzed during the current study.

ORCID

Lei Qiao https://orcid.org/0000-0001-9922-7595

REFERENCES

1. Wang Y, Gu L, Xu Y, Cao X. Practical tracking control of robot manipulators with continuous fractional-order nonsingular terminal sliding mode. *IEEE Trans Ind Electron*. 2016;63(10):6194-6204.
2. Liu C, Zhao Z, Wen G. Adaptive neural network control with optimal number of hidden nodes for trajectory tracking of robot manipulators. *Neurocomputing*. 2019;350:136-145.
3. Liu C, Wen G, Zhao Z, Sedaghati R. Neural-network-based sliding-mode control of an uncertain robot using dynamic model approximated switching gain. *IEEE Trans Cybern*. 2020;51(5):2339-2346. doi:10.1109/TCYB.2020.2978003
4. Kawamura S, Miyazaki F, Arimoto S. Is a local linear PD feedback control law effective for trajectory tracking of robot motion. Proceedings of the IEEE International Conference on Robotics and Automation; 1988:1335-1340.
5. Wen JT, Murphy SH. PID control for robot manipulators, CIRSSE document 54, Rensselaer Polytechnic Institute, 1990.
6. Alvarez-Ramirez J, Cervantes I, Kelly R. PID regulation of robot manipulators: stability and performance. *Syst Control Lett*. 2000;41(2):73-83.
7. Choi Y, Chung WK, Suh IH. Performance and H_∞ optimality of PID trajectory tracking controller for Lagrangian systems. *IEEE Trans Robot Autom*. 2001;17(6):857-869.
8. Slotine JJE, Li W. On the adaptive control of robot manipulators. *Int J Robot Res*. 1987;6(3):49-59.
9. Whitcomb LL, Rizzi AA, Koditschek DE. Comparative experiments with a new adaptive controller for robot arms. *IEEE Trans Robot Autom*. 1993;9(1):59-70.
10. Kelly R, Santibáñez V, Reyes F. A class of adaptive regulators for robot manipulators. *Int J Adapt Control Signal Process*. 1998;12(1):41-62.
11. Galicki M. An adaptive regulator of robotic manipulators in the task space. *IEEE Trans Automat Contr*. 2008;53(4):1058-1061.
12. Wang H, Zhu S, Liu S. Adaptive PID control of robot manipulators with H_∞ tracking performance. Proceedings of the IEEE/ASME International Conference on Advanced Intelligent Mechatronics; 2009:1515-1520; Singapore, Asia.
13. Xu J, Qiao L. Robust adaptive PID control of robot manipulator with bounded disturbances. *Math Probl Eng*. 2013;2013:535437.
14. He W, Huang H, Ge SS. Adaptive neural network control of a robotic manipulator with time-varying output constraints. *IEEE Trans Cybern*. 2017;47(10):3136-3147.
15. He W, Huang B, Dong Y, Li Z, Su C. Adaptive neural network control for robotic manipulators with unknown deadzone. *IEEE Trans Cybern*. 2017;48(9):2670-2682.
16. Zhao K, Song Y. Neuroadaptive robotic control under time-varying asymmetric motion constraints: a feasibility-condition-free approach. *IEEE Trans Cybern*. 2018;50(1):15-24.
17. He W, Mu X, Zhang L, Zuo Y. Modeling and trajectory tracking control for flapping-wing micro aerial vehicles. *IEEE/CAA J Automat Sin*. 2020;8(1):148-156.
18. Zhao K, Lei T, Lin T, Chen L. Robust adaptive fault-tolerant quantized control of nonlinear systems with constraints on system behaviors and states. *Int J Robust Nonlinear Control*. 2020;30(8):3215-3233.
19. Jin X. Adaptive finite-time tracking control for joint position constrained robot manipulators with actuator faults. Proceedings of the American Control Conference; 2016:6018-6023; Boston, MA.
20. He W, Wang T, He X, Yang L, Kaynak O. Dynamical modeling and boundary vibration control of a rigid-flexible wing system. *IEEE/ASME Trans Mechatron*. 2020;25(6):2711-2721.
21. Jin X, Xu JX. A barrier composite energy function approach for robot manipulators under alignment condition with position constraints. *Int J Robust Nonlinear Control*. 2014;24(17):2840-2851.
22. Jin X. Iterative learning control for non-repetitive trajectory tracking of robot manipulators with joint position constraints and actuator faults. *Int J Adapt Control Signal Process*. 2017;31(6):859-875.
23. Wang Y, Li B, Yan F, Chen B. Practical adaptive fractional-order nonsingular terminal sliding mode control for a cable-driven manipulator. *Int J Robust Nonlinear Control*. 2019;29(5):1396-1417.
24. Wang Y, Yan F, Zhu K, Chen B, Wu H. A new practical robust control of cable-driven manipulators using time-delay estimation. *Int J Robust Nonlinear Control*. 2019;29(11):3405-3425.
25. Baek J, Kwon W, Kang C. A new widely and stably adaptive sliding-mode control with nonsingular terminal sliding variable for robot manipulators. *IEEE Access*. 2020;8:43443-43454.
26. Fateh S, Fateh MM. Adaptive fuzzy control of robot manipulators with asymptotic tracking performance. *J Control Automat Electr Syst*. 2020;31(1):52-61.
27. Yu X, He W, Li H, Sun J. Adaptive fuzzy full-state and output-feedback control for uncertain robots with output constraint. *IEEE Trans Syst Man Cybern Syst*. 2021;51(11):6994-7007. doi:10.1109/TSMC.2019.2963072

28. Gao Z. Scaling and bandwidth-parameterization based controller tuning. Proceedings of the American Control Conference; 2003:4989-4996; Denver, CO.
29. Zheng W, Chen M, Zhu R, Mei R. Tracking control of two DOF manipulator based on LADRC. Proceedings of the IEEE 4th International Conference on Advanced Robotics and Mechatronics; 2019:220-225; Toyonaka, Japan.
30. Chen WH, Ballance DJ, Gawthrop PJ, O'Reilly J. A nonlinear disturbance observer for robotic manipulators. *IEEE Trans Ind Electron*. 2000;47(4):932-938.
31. Dai Y, Shi SJ. Globally stable robust adaptive PD+feedforward controller for robot manipulators. *Acta Automat Sin*. 2002;28(1):11-18.
32. Su CY, Leung TP. A sliding model controller with bound estimation for robotic manipulators. *IEEE Trans Robot Autom*. 1993;9(2):208-214.
33. Stepanenko Y, Cao Y, Su CY. Variable structure control of robotic manipulator with PID sliding surfaces. *Int J Robust Nonlinear Control*. 1998;8(1):79-90.
34. Huang H, Zhang T, Yang C, Chen CLP. Motor learning and generalization using broad learning adaptive neural control. *IEEE Trans Ind Electron*. 2019;67(10):8608-8617.
35. Yang C, Jiang Y, Na J, Li Z, Cheng L, Su C. Finite-time convergence adaptive fuzzy control for dual-arm robot with unknown kinematics and dynamics. *IEEE Trans Fuzzy Syst*. 2018;27(3):574-588.

How to cite this article: Qiao L, Zhao M, Wu C, Ge T, Fan R, Zhang W. Adaptive PID control of robotic manipulators without equality/inequality constraints on control gains. *Int J Robust Nonlinear Control*. 2021;1-19. doi: 10.1002/rnc.5849